Diversity and Distributions, (Diversity Distrib.) (2016) 22, 944–959

Diversity and Distributions
A Journal of Conservation Biogeography

BIODIVERSITY RESEARCH

Microclimate predicts within-season distribution dynamics of montane forest birds

Sarah J. K. Frey[1]*, Adam S. Hadley[1,2] and Matthew G. Betts[1]

[1]*Forest Biodiversity Research Network, Department of Forest Ecosystems & Society, Oregon State University, Corvallis, OR 97331, USA,* [2]*Department of Ecology & Evolutionary Biology, University of Toronto, Mississauga, ON, L5L 1C6, Canada*

ABSTRACT

Aim Climate changes are anticipated to have pervasive negative effects on biodiversity and are expected to necessitate widespread range shifts or contractions. Such projections are based upon the assumptions that (1) species respond primarily to broad-scale climatic regimes, or (2) that variation in climate at fine spatial scales is less relevant at coarse spatial scales. However, in montane forest landscapes, high degrees of microclimate variability could influence occupancy dynamics and distributions of forest species. Using high-resolution bird survey and under-canopy air temperature data, we tested the hypothesis that the high vagility of most forest bird species combined with the heterogeneous thermal regime of mountain landscapes would enable them to adjust initial settlement decisions to track their thermal niches.

Location Western Cascade Mountains, Oregon, USA.

Methods We used dynamic occupancy models to test the degree to which microclimate affects the distribution patterns of forest birds in a heterogeneous mountain environment. In all models we statistically accounted for vegetation structure, vegetation composition and potential biases due to imperfect detection of birds. We generated spatial predictions of forest bird distributions in relation to microclimate and vegetation structure.

Results Fine-scale temperature metrics were strong predictors of bird distributions; effects of temperature on within-season occupancy dynamics were as large or larger (1–1.7 times) than vegetation effects. Most species (86.7%) exhibited apparent within-season occupancy dynamics. However, species were almost as likely to be warm associated (i.e., apparent settlement at warmer sites and/or vacancy at cooler sites; 53.3% of species) as cool associated (i.e., apparent settlement at cooler sites and/or vacancy at warmer sites; 46.7% of species), suggesting that microclimate preferences are species specific.

Main conclusions High-resolution temperature data increase the quality of predictions about avian distribution dynamics and should be included in efforts to project future distributions. We hypothesize that microclimate-associated distribution patterns may reflect species' potential for behavioural buffering from climate change in montane forest environments.

Keywords

dynamic occupancy models, forest bird distributions, forest structure and composition, microclimate, mountains, within-season movements.

*Correspondence: Sarah J. K. Frey, Forest Biodiversity Research Network, Department of Forest Ecosystems & Society, Oregon State University, Corvallis, OR 97331, USA.
E-mail: sarah.frey@oregonstate.edu

INTRODUCTION

Climate change is already exerting a strong influence on species range shifts and population trends (Parmesan & Yohe, 2003; Both *et al.*, 2006; Hitch & Leberg, 2007; Devictor *et al.*, 2008; Gutiérrez Illán *et al.*, 2014). Climate change has also been implicated in inconsistent phenological changes across taxa resulting in the decoupling of trophic interactions (Both

DOI: 10.1111/ddi.12456
http://wileyonlinelibrary.com/journal/ddi

& Visser, 2005). Given that such deviations are expected to amplify over the coming century (IPCC, 2014), a key question is the degree to which biodiversity will be affected as a result (Thomas *et al.*, 2004).

Making reliable predictions about species' responses to climate change has been challenging because responses have not been uniform; empirical studies using historical datasets have revealed high among-species variation in the degree to which populations and species distributions respond over time (Tingley *et al.*, 2012; Gutiérrez Illán *et al.*, 2014). Although some species demonstrate range shifting in response to climate change (Tingley & Beissinger, 2009; Virkkala *et al.*, 2014), many species have not extended their ranges to occupy the geographic extent of apparently 'suitable' climates, either historically (Araújo & Pearson, 2005; Moritz & Agudo, 2013) or during recent rapid climate change (Thuiller *et al.*, 2004b). Although some of this variation in species responses is associated with life-history traits (Sheldon *et al.*, 2011), much variation remains unexplained.

One hypothesis for this mismatch between climate envelope predictions and observed responses to change is that climate data used to define suitable envelopes are collected at resolutions much coarser than those perceived and used by organisms in habitat selection (Pearson & Dawson, 2003; Logan *et al.*, 2013; Storlie *et al.*, 2014). Most temperature data are collected at scales 10^4-fold larger than the territory sizes of focal organisms (Potter *et al.*, 2013), and there is high potential for hidden microclimate variation within broader regional patterns (Franklin *et al.*, 2013). Climate is assumed to be mainly a driver of distribution patterns at broad spatial scales (Thuiller *et al.*, 2004a; Boucher-Lalonde *et al.*, 2014) although habitat characteristics such as vegetation structure and composition are thought to overwhelm the importance of climate at finer spatial scales (Brown, 1995; Luoto *et al.*, 2007). Therefore, this hidden microclimatic variation and its potential to affect distribution dynamics are often overlooked (Huey *et al.*, 2012; Cumming *et al.*, 2014). Additionally, lack of high-resolution climate data, particularly under-canopy temperatures (Scherrer *et al.*, 2011), has prohibited effective testing of the role of microclimate in fine-scale distribution dynamics.

Environmental heterogeneity offers a range of resources and microclimates that can provide options for 'microrefugia' where an organism can persist in the face of regional warming (Keppel *et al.*, 2012; Patsiou *et al.*, 2013). In addition, microclimate variability at fine spatial scales could provide options for short-distance, adaptive movements and resource tracking within a season (Karr & Freemark, 1983; Dobrowski, 2010). Animals may adjust their use of local habitat in ways that allow them to persist in the face of climate change without necessitating broad-scale range shifts (Kearney *et al.*, 2009). Landscapes with little climatic variability provide fewer possibilities for new behaviour (Bonebrake *et al.*, 2014) such as shifts in habitat or diet.

Direct tracking of individual behaviour to examine within-season movements (e.g., Gow & Stutchbury, 2013) is logistically challenging, particularly when considering more than a single species. However, dynamic occupancy modelling offers a viable alternative for quantifying within-season distribution changes (MacKenzie *et al.*, 2003). These models allow changes in colonization and extinction processes across a season and have been shown to outperform static occupancy models for many species (McClure & Hill, 2012). Recent work has demonstrated that within-season movements by birds may actually be relatively common (McClure & Hill, 2012; Gow & Stutchbury, 2013), which violates the assumptions of commonly used species' occupancy models (Rota *et al.*, 2009) and necessitates the application of dynamic models. Within-season movements appear to reflect shifts to higher quality sites (Betts *et al.*, 2008; Gilroy *et al.*, 2010) and often represent shifts upwards along elevational gradients (Brambilla & Rubolini, 2009). Given that site quality may change over the breeding season as temperatures warm (Vatka *et al.*, 2011), being sufficiently flexible to take advantage of new favourable microclimates should be adaptive and allow birds to track their thermal niches across space and time. Within-season occupancy dynamics are thought to represent a combination of two important processes: (1) true settlement and vacancy (i.e., birds settling in or shifting away from territories) and (2) temporary immigration/emigration in and out of sampling locations due to the combination of (1) variation in territory density and (2) territories not always falling completely within the sampling radius (Chandler *et al.*, 2011). As both of these processes result from movement at either fine or broad spatial scales due to variation in habitat suitability (i.e., settlement, disproportionate within-territory use, and higher territory densities should all be associated with favoured sites), it is possible to use a dynamic occupancy framework to examine habitat suitability for multiple species across a landscape.

In both 2012 and 2013, we sampled a forest bird community six times during the breeding season at 183 sites in complex mountainous terrain, resulting in 19,171 bird observations. We collected under-canopy temperature data with sensors located at each of the count sites (Frey *et al.*, 2016). We used dynamic occupancy modelling to test the relative roles of fine-scale temperatures and vegetation characteristics on within-season distribution dynamics while accounting for imperfect detection. We hypothesized that high vagility of most forest bird species, combined with the heterogeneous thermal regime of mountain landscapes, would enable within-season distribution dynamics such that birds can track their thermal niches.

METHODS

Study design

We collected bird occurrence data at 183 sample locations within the H. J. Andrews Experimental Forest (HJA). The 6400-ha HJA spans an elevational gradient from 410 to 1630 m.a.s.l. and is located in the western Cascades of Oregon, USA (44°12′ N, 122°15′ W, Fig. S2a). It is a forest mosaic comprising a mix of old-growth forest, mature forests, ~60-year-old Douglas-fir (*Pseudotsuga menzisii*) plantations, alpine meadows, Sitka alder (*Alnus viridis*) or vine maple (*Acer circinatum*) shrub fields, and landslides (Fig. S2b).

We used a stratified, systematic, random design to select sample locations. We stratified across elevation, distance to road and habitat type (plantation or mature/old-growth forest). Distance between all sampling points was ≥300 m to avoid double sampling. Sample points were categorized as transect, trail or road. Transect points were selected by placing a systematic grid of points across a portion of the watershed using GIS (ESRI, 2011). We separated each transect by 600 m. We placed trail points randomly along existing and abandoned trails (<1 m wide) at 300-m intervals. To select road points, we first placed points randomly along maintained and abandoned gravel roads at 600-m intervals using Hawth's tools (Beyer, 2004). Then, we chose a random direction and distance from the road into the forest (0, 50, or 100 m) for the final point placement. Our final dataset was comprised of 60 transect points, 68 road points and 55 trail points.

Point counts

We conducted point counts on six separate occasions from 14 May to 9 July in 2012 and from 14 May to 10 July in 2013, which corresponded to spring arrival and subsequent breeding period for the majority of bird species at HJA. Point counts were conducted during favourable weather conditions by trained observers. The mean (SD) length of sample occasions was 5 (1.17) and 6 (1.22) days in 2012 and 2013, respectively. Mean (SD) break length between point count rounds was 4 (1.91) days in 2012 and 5 (1.90) days in 2013. Surveys occurred between 05:15 h and 10:30 h and each consisted of a 10-min point count where we recorded all birds seen or heard within a 100-m radius. Each 10-min point count was divided into three 3-min 20-s subcounts where the point count was reinitiated (see Betts *et al.*, 2008 for methods details). We detected a total of 41 species during May–July 2012 and 2013; however, we did not use data from species with <0.2 prevalence because models in these cases often failed to converge. Thus, we modelled occupancy dynamics of 15 species (Table 1).

Environmental covariates

We placed data loggers (Onset HOBO Pendant Temperature/Light Data Logger 64K, model UA-002-64 [*n* = 167] and Onset HOBO Water Temperature Pro v2 Data Logger, model U22-001 [*n* = 16]) that recorded temperature every 20 min at each sample point. We summarized temperature measurements between January 2012 and December 2013 (see Appendix S1 and Frey *et al.*, 2016 for details on logger placement and data processing). We used five temperature metrics that we expected to influence forest birds during the breeding season and/or alter timing of important phenological events upon which birds depend. These metrics included cumulative degree days (CDD) >0 °C January–March and >10 °C April–June, both of which are expected to be important drivers of bud break and insect abundance (Fu *et al.*, 2012), bird phenology (Both *et al.*, 2005) and bird distributions (Araújo *et al.*, 2005). We included mean monthly temperatures (monthly mean, maximum and minimum) from April to June. Mean maximum and mean minimum monthly temperatures capture temperature extremes and have been used to describe avian distributional boundaries (Root, 1988)

Table 1 Species list for the 15 bird species we examined at the H. J. Andrews Experimental Forest. Prevalence (Prev.) is the number of points for which a species was detected at least once throughout the breeding season out of the total points (183) for each year. Home range values were obtained from the online Birds of North America accounts (Poole, 2005). Thermal preference (pref.) is based on model results (see *Results* section).

Species' common name	Species' scientific name	Species code	Prev. 2012	Prev. 2013	Home range (ha)	Thermal pref.
Brown creeper	*Certhia americana*	BRCR	0.435	0.495	4.2	Warm
Chestnut-backed chickadee	*Poecile rufescens*	CBCH	0.913	0.826	1.3	Warm
Golden-crowned kinglet	*Regulus satrapa*	GCKI	0.674	0.647	1.6	Cool
Hammond's flycatcher	*Empidonax hammondii*	HAFL	0.386	0.446	1	Warm
Hermit thrush	*Catharus guttatus*	HETH	0.462	0.527	0.7	Cool
Hermit warbler	*Setophaga occidentalis*	HEWA	0.875	0.951	0.35	Cool
Oregon junco	*Junco hyemalis*	ORJU	0.620	0.663	0.38	Cool
Pacific wren	*Troglodytes pacificus*	PAWR	0.821	0.793	1.38	Warm
Pacific-slope flycatcher	*Empidonax difficilis*	PSFL	0.761	0.853	2.5	Warm
Red-breasted nuthatch	*Sitta canadensis*	RBNU	0.511	0.783	1.2	Cool
Steller's jay	*Cyanocitta stelleri*	STJA	0.630	0.625	80	Warm
Swainson's thrush	*Catharus ustulatus*	SWTH	0.674	0.723	1	Warm
Varied thrush	*Ixoreus naevius*	VATH	0.609	0.565	7	Cool
Western tanager	*Piranga ludoviciana*	WETA	0.277	0.342	2.8	Warm
Wilson's warbler	*Cardellina pusilla*	WIWA	0.299	0.266	0.3	Cool

and predict abundance trends (Gutiérrez Illán *et al.*, 2014). Mean monthly temperature describes the general temperature conditions at a site and is a common metric in species-climate studies (Virkkala *et al.*, 2008; Stralberg *et al.*, 2009). We chose the months of April, May and June since this is the period when we expected the majority of within-breeding season dynamics to take place.

To describe vegetation structure at each of our sites, we used LiDAR-derived metrics and a principal component analysis (PCA, Appendix S2, Table S1, Frey *et al.*, 2016). We used the first two components in our analysis as they explained 75% of the variability in our structure metrics (PC1 = 45%, PC2 = 30%, Table S2). We quantified forest composition by measuring the proportion of deciduous basal area at a site using variable radius prism plots and counting deciduous trees and large shrubs >2 cm DBH (see Table S3 for species list). We chose deciduous vegetation as our composition variable because it is often associated with abundance of leaf-gleaning forest birds and deciduous plant species are typically thought to support higher abundances of insects (Hagar, 2007; Ellis & Betts, 2011).

Occupancy models

We used dynamic occupancy models (MacKenzie *et al.*, 2003) to estimate within-season distribution dynamics as a function of microclimate conditions in the HJA. These models use detection histories from multiple surveys (i.e., our three subcounts) over multiple seasons (i.e., six site visits) to estimate four parameters: (1) detection probability (p), (2) initial site occupancy (ψ), (3) site colonization (γ) and (4) local-site extinction (ε). Occupancy models are hierarchical in that they model the observation process (detection) independent from the ecological processes of interest (site occupancy, colonization and extinction; see Appendix S3 for model structure). For our within-season application of dynamic occupancy models, we refer to colonization as site 'settlement' (γ) and extinction as site 'vacancy' (ε). We modelled 2012 and 2013 separately for simplicity in model structure (testing for year effects would result in at least an additional nine model parameters).

The resulting parameter estimates for colonization/extinction stem from the combined processes of true settlement/vacancy (i.e., birds settling in or shifting away from sites) and temporary immigration/emigration in and out of the point count circle. For example, species with larger home ranges may be more likely to move out of a count circle while remaining within their original home ranges. In instances with large home ranges, within-territory/home-range movements could cause the appearance that a territory has become vacant when the bird is actually still within its initial home range (i.e., the territory is counted as vacant when it is not). Similarly, in areas of high density, multiple territories could overlap the count circle and the likelihood of detecting at least one individual within the count circle is higher, purely because more individuals are present.

We addressed the role of temporary within-territory movements in estimates of occupancy dynamics in two ways. First, we used information about the average home range size for each species (Table 1, Poole, 2005) to test whether species with larger home ranges show higher levels of within-season dynamics. Higher levels of dynamics for species with larger home ranges would suggest artificially high apparent settlement and vacancy rates due simply to within-home range movements (Betts *et al.*, 2008). Secondly, we used detections within a 100-m radius to increase the likelihood that entire territories were included within the boundaries of the sample plot. The majority of species (12/15) we included in our study have territory sizes that are smaller than our sample plot (Table 1, area of 100-m radius point count circle = 3.14 ha).

Model selection

We selected survey- and site-level covariates we expected to be important in our system *a priori* (see *Environmental covariates* above). In order to reduce our model set, we used a manual forward stepwise approach to select the variables that best explained detection and site occupancy parameters (Chandler & King, 2011). All continuous predictor variables were standardized (z-transformed) to enable comparison of effect sizes. We compared support for models containing different covariates using AIC (Burnham & Anderson, 2002).

The objective of the model selection process was to select the best temperature metric for each parameter while also including important vegetation variables. Our model selection steps for each parameter were as follows: (1) We first ranked univariate models for each of the covariates using AIC. (2) We then constructed additive models including covariates in order of their AIC ranking (highest to lowest). We added variables in order of support until additional covariates resulted in the model being >2 ΔAIC points below the top model. (3) We selected the most parameterized model within 2 AIC points of the top model (this was often the top-ranked model; i.e., ΔAIC = 0). We combined top-ranked temperature and vegetation metrics in additive models. We did include multiple vegetation variables in the same model when there was support for more than one. However, we never combined multiple temperature metrics in any additive models due to intervariable correlation (Table S4). We chose not to use model averaging because it is not recommended for competing models that contain correlated variables (Cade, 2015).

We tested for differences in detection as a function of eight temperature and vegetation variables and six survey-level variables (i.e., survey time, day of year [days since May 1], observer, stream noise, weather conditions [cloud cover and wind] and a temporal autocovariate). We included temperature metrics as covariates for detection to avoid potentially attributing effects of temperature to changes in distributions when, in actuality, they were due to detectability. Also, a site's thermal regime could influence detection through higher or lower activity levels of birds (which would in turn affect how easily we detect them) at sites that are generally warmer or cooler. We included a temporal autocovariate because subcounts were temporally autocorrelated. This autocovariate indicated whether an individual was detected in the previous subcount. We then used forward stepwise selection as described above to determine the best detection model.

We compared univariate models of our microclimate and vegetation metrics while holding the other dynamic parameter constant (i.e., vacancy was modelled as the mean across all sites while examining settlement and vice versa). We then combined the top variables for both settlement and vacancy to obtain the final model. We created spatial maps of bird distributions as a function of the temperature and vegetation structure variables using the final models (see Appendix S4 for methods). To determine whether the effects of temperature depended on vegetation and vice versa, we tested for interactions between the most-supported temperature and vegetation variables in the final models. All analyses were conducted in R version 3.1.1 (R Development Core Team, 2011) using the 'unmarked' package (Fiske & Chandler, 2011).

Relative importance of microclimate and vegetation

Once we identified the top models for each of the 15 species in each year, we assessed relative importance of the temperature and vegetation metrics using the effect sizes. To account for differences in precision of effect sizes, we divided these by the corresponding standard errors (Ritchie *et al.*, 2009). When more than one vegetation metric was in the top model, we selected, for comparison, the one with the largest effect size. In the rare instance where none of the metrics were useful in explaining variability in occupancy parameters, we considered the effect size to be zero. We did this for initial occupancy, settlement and vacancy.

Model fit

We used parametric bootstrapping to evaluate the goodness-of-fit of the best model for each species in each year (Kéry & Chandler, 2012). For each species, we simulated 250 datasets from its top model in a given year. Each time we refitted the model to these simulated data, we computed a fit statistic (sum of squares error [SSE]). The simulation resulted in a reference distribution of the fit statistic from which we computed a *P*-value indicating the proportion of the reference distribution that was greater than the observed value. We used χ^2 to compare observed and expected fit statistics because it has been shown to perform well at evaluating goodness-of-fit for logistic regression models (Hosmer *et al.*, 1997; MacKenzie & Bailey, 2004; Kéry & Chandler, 2012). Models with fit statistics that are higher than the mean from the simulated distribution are indicative of overdispersion in the data, meaning that there is still unexplained variability.

Spatial autocorrelation, a common property of ecological data, could potentially be problematic due to violation of sample independence assumptions (Legendre, 1993). Therefore, we tested for spatial autocorrelation in our data by calculating Moran's *I* for the residuals from the top model for each species. Moran's *I* values can range from 0 to 1, and values >0.3 are considered relatively large (Lichstein *et al.*, 2002).

RESULTS

Overall, temperature and vegetation metrics were strong predictors of initial bird distributions (Fig. 1, Table S5). Temperature was the most important predictor (largest effect size) for 80% and 47% of species in 2012 and 2013, respectively. Of the species with temperature as an important predictor (95% confidence interval did not overlap 0) in the top model (Fig. 1), roughly equal numbers were associated with warm sites (53%) versus cooler sites (47%) in both years (Table S5). Vegetation (structure and/or composition) was an important predictor of initial occupancy patterns for a substantial proportion of species in both years (2012: 33%, 2013: 47% of species, Fig. 1, Table S5) and was more important than temperature for 20% and 53% of species in 2012 and 2013, respectively. For most species, detection probability was explained well by survey (temporal autocovariate, time of day, day of year and stream noise; Table S6) and site (temperature and vegetation; Table S7) covariates.

In both years, the majority of species showed mean settlement and vacancy rates >0.1 throughout the breeding season indicating that overall occupancy patterns were dynamic (Table S8; settlement – 80.0% of species in both years;

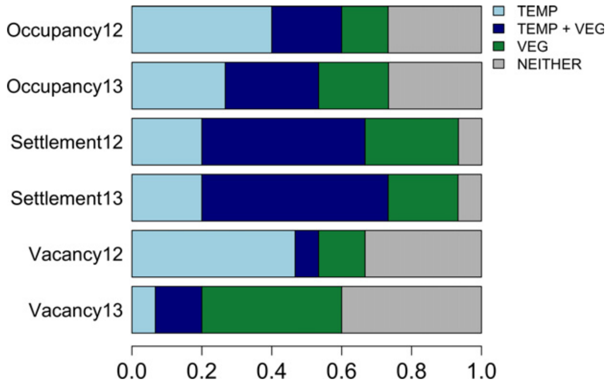

Figure 1 The proportion of species in each year for each of the ecological parameters where the effects of (1) temperature alone (TEMP), (2) both vegetation and temperature (BOTH) or (3) vegetation alone (VEG) were important (95% CIs did not overlap 0) in the top model, or whether (4) neither vegetation nor temperature (TEMP + VEG) was important in the top model. Initial occupancy described the distribution in the first sample session (mid-May). Settlement and vacancy described distribution dynamics between the second and sixth sample sessions (late May until early July).

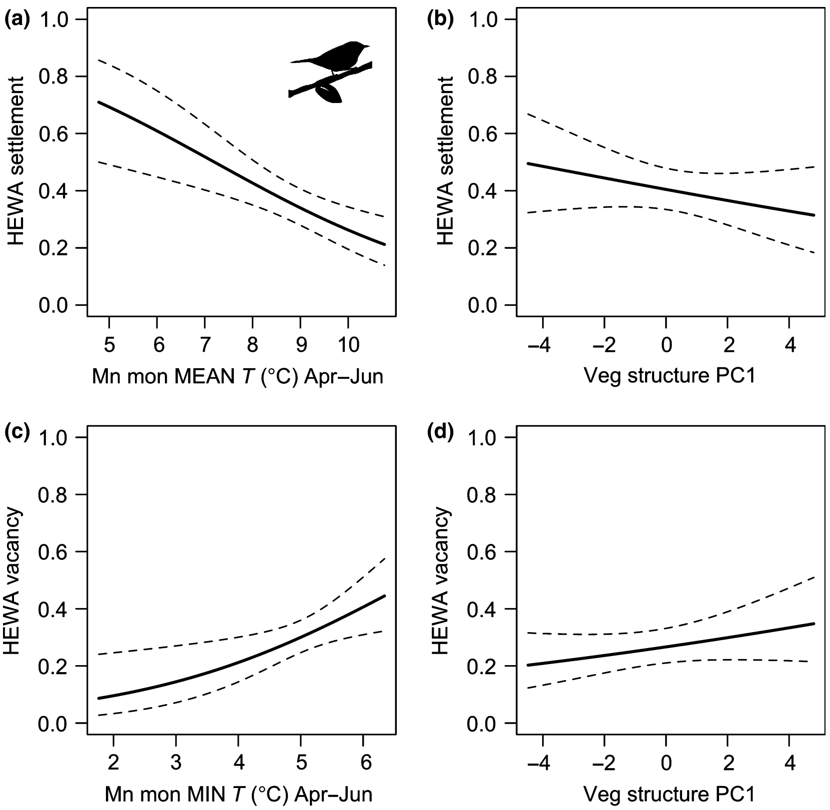

Figure 2 Hermit warbler (*Setophaga occidentalis*, HEWA) is an example of a species where site-level dynamics are largely driven by temperature and vegetation structure to a lesser extent. Hermit warblers were both less likely to settle sites (a) and more likely to vacate sites (c) that were warmer. Vegetation structure was not an important predictor of either vacancy (b) or settlement (d). Mn, mean; mon, monthly; T, temperature; Veg, vegetation; PC, principal component; MIN, minimum.

vacancy – 2012: 86.7%, 2013: 93.3%). On average for all species, mean vacancy probability (mean [SD] – 2012: 0.39 [0.20], 2013: 0.38 [0.21]) tended to be higher than settlement probability (2012: 0.22 [0.14], 2013: 0.22 [0.13]). The mean settlement and vacancy rates are interpreted as the change in occupancy that occurred between each sampling occasion (i.e., between 1 and 2, 2 and 3, etc.), on average, across all sites (not including any covariate effects).

Site-level temperature metrics were strong predictors of the apparent distribution changes we observed, and temperature was equal or more effective (1–1.7 times) than vegetation at predicting local-site occupancy dynamics in both years (Figs. 1-5, Tables 2, 3 and S9). Temperature metrics were the most important predictors (larger effect sizes) for at least one dynamic parameter for 73.3% and 66.7% of species in 2012 and 2013, respectively (see Tables 2 and 3 for coefficients from top models, and see Table S9 for comparison of SE-adjusted effect sizes). Overall, species were almost as likely to be cool associated (i.e., higher apparent settlement at cooler sites and/or vacancy at warmer sites; 53.3% of species, Figs. 2 & 3) as warm associated (i.e., higher apparent settlement at cooler sites and/or vacancy at warmer sites; 46.7% of species; Figs. 4 & 5, Table 1). Preference for cool versus warm sites never switched between years for a species for any of the ecological parameters (Tables 2 and 3, Figs. S3 & S4). However, whether the effects of temperature alone, vegetation alone or both were most important for a given parameter varied within species between years. For species whose apparent settlement patterns were largely temperature driven, 71.4% (2012) and 62.5% (2013) showed preference for sites with cooler microclimates (Table 2, Fig. S3). For species whose vacancy patterns were driven primarily by temperature, 77.8% (2012) and 55.6% (2013) were those that vacated warmer sites (Table 3, Fig. S4). We found little support for temperature–vegetation interactions (Table S11).

Our goodness-of-fit tests indicated no, or minimal lack of fit due to overdispersion in our models (Table S10). Goodness-of-fit tests for Steller's jay in 2012 and hermit thrush in 2013 suggested slight overdispersion ($P = 0.33$ and 0.11, respectively). Three species (only in 2012) showed little to no difference between the observed and mean expected fit statistic ($0.25 < P < 0.75$). We did find evidence for underdispersion in our data; the majority of species had fit statistics that were lower than the distribution of bootstrapped values ($P > 0.75$). Underdispersion is generally not considered a problem as it results in inflated standard errors, leading to more conservative estimates of covariate effects (Hosmer *et al.*, 2013). Further, we found no evidence for spatial autocorrelation in the residuals (mean [SD] Moran's I for all species $2012 = -0.002$ [0.014], $2013 = 0.001$ [0.007]; mean [SD], P-values $2012 = 0.230$ [0.046], $2013 = 0.237$ [0.031]) indicating that spatial autocorrelation was not prevalent in our study (Table S9).

DISCUSSION

Forest bird distributions in our study responded strongly to fine-scale thermal conditions. Climate is widely accepted to

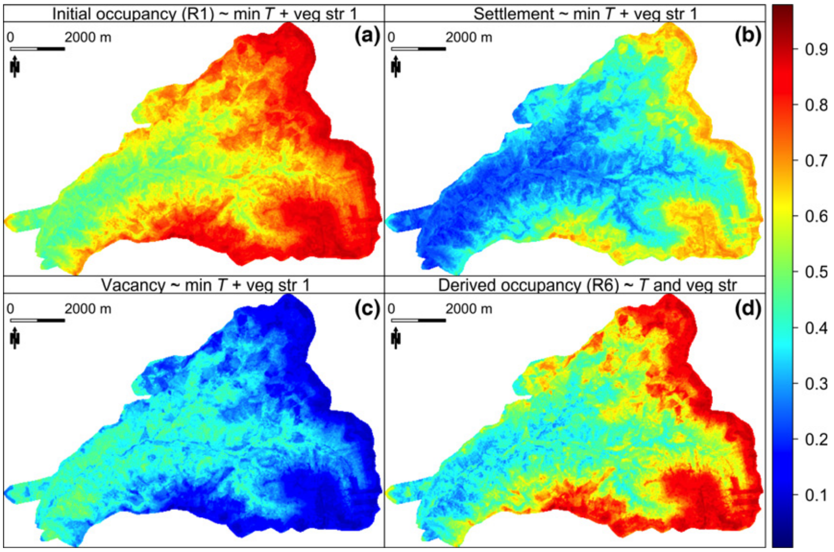

Figure 3 Predicted maps for hermit warbler (a) initial occupancy, (b) settlement, (c) vacancy and (d) final occupancy patterns at the end of the sampling period. Hermit warblers show higher apparent vacancy at warmer sites and higher apparent settlement at cooler sites. By the end of the season, (d) hermit warblers have shifted away from warmer sites towards cooler sites. The Andrews Forest is low elevation to the east and high elevation to the west (see Fig. S2 for elevation and canopy height distributions). T, temperature; veg str 1, vegetation structure variable PC1; mn, mean; min, minimum; R1, round 1 of point counts; R6, round 6 of point counts.

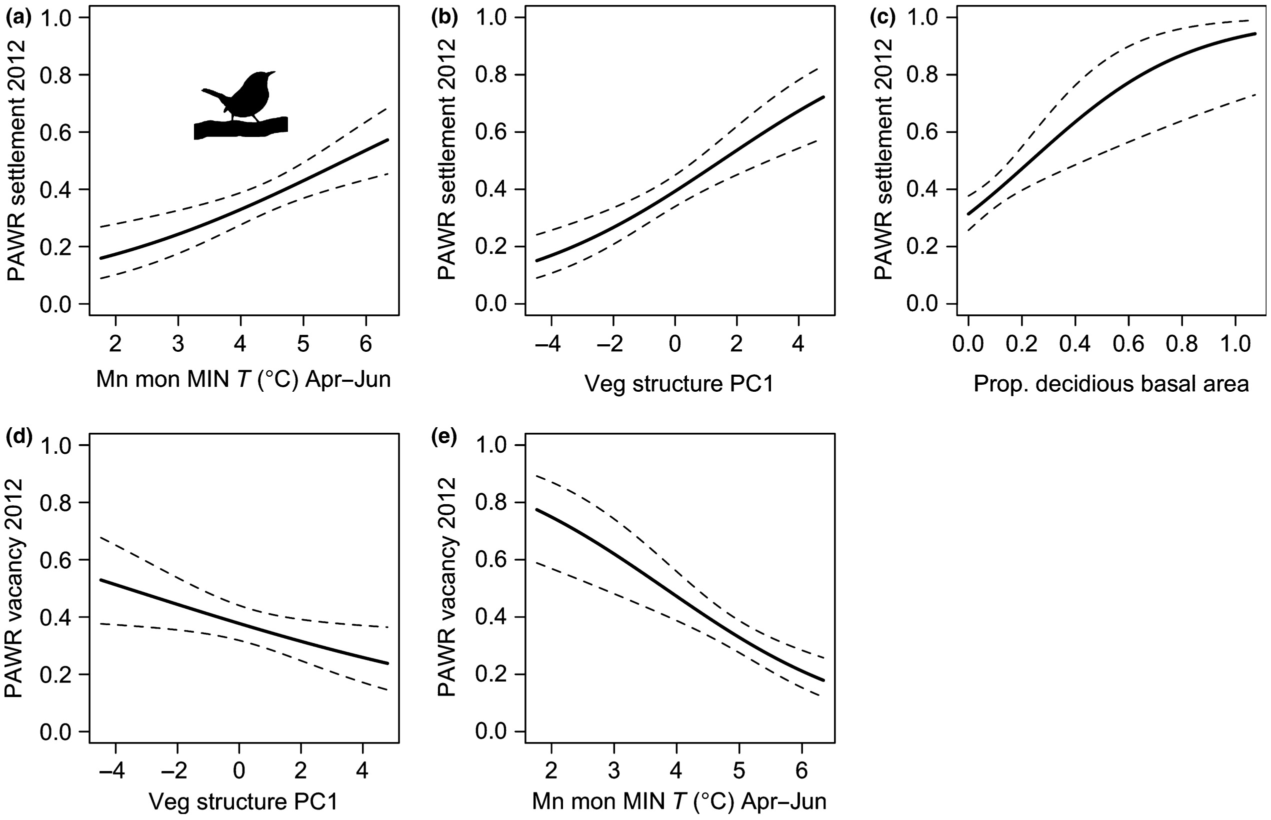

Figure 4 Pacific wren (*Troglodytes pacificus*, PAWR) is an example of a warm-associated species where both temperature and vegetation were important in within-season dynamics. Pacific wrens were more likely to settle warmer sites (a) and vacate cooler sites (e). Pacific wrens were more likely to settle sites with old-growth characteristics (b) and higher deciduous composition (c). Wrens were more likely to vacate even-aged vegetation stands such as plantations (d). Mn, mean; mon, monthly; MIN, minimum; T, temperature; Veg, vegetation; PC, principal component; Prop, proportion.

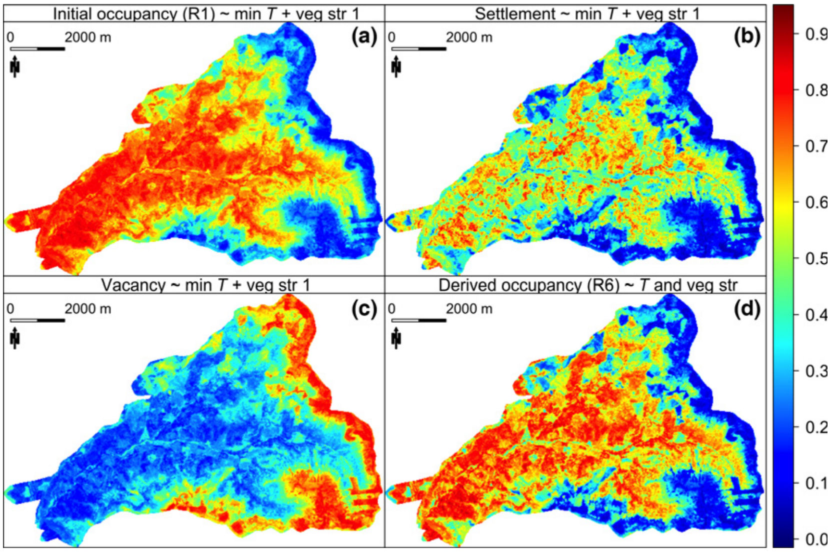

Figure 5 Predicted distribution maps for Pacific wren (a) initial occupancy, (b) settlement, (c) vacancy and (d) final occupancy patterns at the end of the sampling period. By the end of the season, (d) Pacific wrens have shifted away from plantation sites towards older forest sites. The predicted maps for this species highlight the strong vegetation component in addition to temperature. Maps do not include proportion of deciduous basal area since it is a local-site vegetation variable. The Andrews Forest is low elevation to the east and high elevation to the west (see Fig. S2 for elevation and canopy height distributions). T, temperature; veg str 1, vegetation structure variable PC1; min, minimum; R1, round 1 of point counts; R6, round 6 of point counts.

be a major driver of species distributions at broad spatial extents (Thuiller *et al.*, 2004a; Thomas, 2010; Boucher-Lalonde *et al.*, 2014), but to our knowledge, this is the first evidence of fine-scale temperature effects on bird occupancy dynamics. Local habitat selection in birds has often been shown to depend on vegetation characteristics (Hildén, 1965) such as structure (MacArthur *et al.*, 1962; Seavy *et al.*, 2009) and composition (Ellis & Betts, 2011). However, local-scale temperature appears to be of equal or possibly greater importance than vegetation in site selection by forest birds in our system. Clearly our findings do not downplay the important role of vegetation in species distributions; rather, they highlight the need to account for microclimate variability when considering distributional changes. Occupancy dynamics for many species we examined depended on both microclimate and vegetation metrics. Although we do not know of any other bird occupancy studies that have compared the role of local-scale temperature and vegetation in a forest system, there is some previous evidence that the combined effects of vegetation and temperature influence avian occurrence patterns in other systems. For example, in an exurban environment, Lumpkin & Pearson (2013) found that both temperature and habitat characteristics (building density and forest cover) affected bird occurrence patterns. Further, previous work conducted at broad spatial scales has shown a strong influence of both vegetation and temperature on bird distributions (Cumming *et al.*, 2014).

Microclimate is known to be important for ectotherms due to thermoregulation requirements (Scheffers *et al.*, 2014), but has only been recently considered for endotherms (Boyles *et al.*, 2011; Long *et al.*, 2014). The influence of climate on endothermic species distributions has been almost exclusively explored at large spatial scales (Peterson *et al.*, 2002; Mitikka *et al.*, 2008), 10^4-fold larger than the scale at which organisms generally make habitat selection decisions (Potter *et al.*, 2013). An important advance in our study was that we directly measured air temperature at the same sites where we counted birds; we did not use elevation as a proxy for temperature (Klemp, 2003; Maggini *et al.*, 2011) or interpolate temperature from widely spaced temperature stations placed in open areas (Scherrer *et al.*, 2011). The combination of dynamic occupancy modelling and high-resolution temperature data allowed us to elucidate clear changes in intra-season distributional patterns for multiple species along a microclimate gradient.

We found that most species of forest birds examined exhibited apparent within-season distribution dynamics. Our results add to growing evidence that within-season site occupancy may be less static than traditionally assumed (Betts *et al.*, 2008; McClure & Hill, 2012). For example, McClure & Hill (2012) also found dynamic occupancy models outperformed static occupancy models in a south-eastern U.S. forest bird community suggesting birds were shifting sites within a breeding season. Radio tracking (Klemp, 2003; Gow & Stutchbury, 2013), territory mapping (Brambilla & Rubolini, 2009) and mark–recapture studies (Gilroy *et al.*, 2010) have also demonstrated within-season movements and site shifts in birds.

Within-season shifts can be the result of three main processes: (1) habitat upgrading, (2) thermoregulation and (3) resource tracking. Shifts are often thought to follow failed breeding attempts (Switzer, 1997; Hoover, 2003) or represent

Table 2 Coefficients (Est) and standard errors (SE) for apparent settlement (γ) as a function of temperature and vegetation (structure and composition) metrics by species and year for top models (see Table 1 for species code definitions and see Appendix S6 for all model selection tables).

			Vegetation						Temperature									
	Intercept		Structure PC1		Structure PC2		Composition		CDD >0 J–M		CDD >10 A–J		Max T A–J		Min T A–J		Mean T A–J	
Species	Est	SE	Est	SE	Est	SE	Est	SE	Est	SE	Est	SE	Est	SE	Est	SE	Est	SE
2012																		
BRCR	−1.90	0.17	0.69	0.17*	−0.19	0.13												
CBCH	0.19	0.19	0.19	0.18	−0.57	0.19*									0.36	0.17*		
GCKI	−1.13	0.11					−0.15	0.13									−0.56	0.11*
HAFL	−2.67	0.29					0.40	0.19*	−0.43	0.34								
HETH	−1.31	0.21	−0.44	0.17*											0.17	0.19		
HEWA	−0.39	0.15	−0.18	0.16													−0.53	0.16*
ORJU	−1.08	0.17	−0.39	0.16*													−0.54	0.19*
PAWR	−0.43	0.12	0.64	0.14*			0.57	0.16*							0.49	0.13*		
PSFL	−0.93	0.11	0.55	0.13*											0.26	0.12*		
RBNU	−1.74	0.27													−0.33	0.29		
STJA	−1.07	0.20	−0.27	0.16†													0.32	0.14*
SWTH	−0.93	0.15	−0.27	0.14*									0.23	0.13†				
VATH	−1.43	0.14			−0.31	0.12*											−0.53	0.13*
WETA	−2.85	0.26			0.54	0.19*					0.90	0.20*						
WIWA	−2.95	0.19	−0.50	0.18*							−0.38	0.17*						
2013																		
BRCR	−1.68	0.18	0.46	0.18*	−0.23	0.14†	−0.34	0.22					−0.27	0.17				
CBCH	−0.64	0.14	0.32	0.15*	−0.37	0.13*									0.28	0.16†		
GCKI	−1.29	0.11			−0.13	0.12											−0.91	0.13*
HAFL	−2.19	0.18	0.47	0.16*													0.22	0.19
HETH	−1.86	0.12	−0.47	0.12*	−0.25	0.12*											−0.32	0.12*
HEWA	−0.03	0.15	−0.43	0.17*			−0.38	0.17*									−0.64	0.16*
ORJU	−1.08	0.13	−0.50	0.14*											−0.57	0.16*		
PAWR	−0.94	0.12	0.56	0.14*											0.55	0.14*		
PSFL	−0.48	0.11	0.43	0.13*											0.44	0.13*		
RBNU	−0.12	0.26			−0.48	0.24*	−0.46	0.23*					−0.54	0.24*				
STJA	−3.27	1.64							1.33	0.92								
SWTH	−1.13	0.12					0.19	0.11†					0.36	0.10*				
VATH	−1.52	0.13			−0.21	0.12†					−0.43	0.12*						
WETA	−2.00	0.25	−0.64	0.16*									0.21	0.15				
WIWA	−3.11	0.30			−0.65	0.26*							−0.42	0.26*				

*95% confidence interval does not overlap 0.

†90% confidence interval does not overlap 0; CDD, cumulative degree days; J–M, January–March; A–J, April–June; T, temperature; PC, principal component.

Table 3 Coefficients (Est) and standard errors (SE) for apparent vacancy (ε) as a function of temperature and vegetation (structure and composition) metrics by species and year for top models (see Table 1 for species code definitions and see Appendix S6 for all model selection tables).

			Vegetation						Temperature									
	Intercept		Structure PC1		Structure PC2		Composition		CDD >0 J–M		CDD >10 A–J		Max T A–J		Min T A–J		Mean T A–J	
Species	Est	SE	Est	SE	Est	SE	Est	SE	Est	SE	Est	SE	Est	SE	Est	SE	Est	SE
2012																		
BRCR	1.13	0.47			0.28	0.28	1.22	0.86										
CBCH	−0.54	0.14	−0.24	0.13†	0.15	0.12			−0.22	0.13†								
GCKI	0.35	0.18			0.10	0.16											0.33	0.16*
HAFL	−0.52	0.39	−0.71	0.41†									−0.61	0.26*				
HETH	0.64	0.30	0.11	0.26											0.69	0.29*		
HEWA	−1.01	0.16	0.18	0.13											0.54	0.21*		
ORJU	0.38	0.26					0.19	0.21							1.32	0.28*		
PAWR	−0.50	0.13	−0.31	0.14*											−0.70	0.16*		
PSFL	−0.39	0.16	−0.26	0.16	0.29	0.13*									−0.24	0.19		
RBNU	−1.22	0.49	0.28	0.36													0.69	0.46
STJA	1.04	0.31					−0.27	0.24	−0.23	0.25								
SWTH	−0.27	0.23	0.20	0.19														
VATH	0.95	0.28	−0.03	0.21									0.65	0.25*				
WETA	0.81	0.47	0.60	0.36†													−0.28	0.36
WIWA	0.90	0.40	0.26	0.28							1.69	0.48*						
2013																		
BRCR	0.30	0.24			0.36	0.21†					−0.36	0.24						
CBCH	−0.57	0.21					−0.63	0.29*									−0.32	0.18†
GCKI	0.23	0.19					0.32	0.17†									0.55	0.17*
HA(SE) FL	−0.34	0.32			−0.42	0.20*											−0.35	0.25
HETH	0.64	0.21	0.34	0.18†													0.15	0.20
HEWA	−0.81	0.10	−0.06	0.10													0.43	0.11*
ORJU	−0.10	0.20	0.02	0.20											0.29	0.18†		
PAWR	−0.69	0.13			0.38	0.12*									−0.52	0.16*		
PSFL	−0.62	0.14	−0.33	0.14*											−0.41	0.17*		
RBNU	−1.05	0.17			0.14	0.15	0.19	0.18									0.23	0.15
STJA (Est)	−2.68	0.63	1.00	0.41*											0.69	0.54		
SWTH	−0.07	0.19			−0.36	0.16*	−0.17	0.16					−0.14	0.18				
VATH	1.05	0.26					−0.40	0.31†							0.39	0.22		
WETA	1.46	0.44													0.29	0.40		
WIWA	−4.66	1.78			−1.13	0.46*	−4.62	2.34*									−1.15	0.74

*95% confidence interval does not overlap 0.

†90% confidence interval does not overlap 0; CDD, cumulative degree days; J–M, January–March; A–J, April–June; T, temperature; PC, principal component.

upgrading along gradients in habitat quality (Betts *et al.*, 2008). Models of habitat selection typically assume that when animals select a breeding site, they possess the necessary ('ideal') information about site quality and dispersal capabilities to make the best choice (Fretwell & Lucas, 1969; Pulliam & Danielson, 1991). In reality, it may not be possible to obtain dependable site quality information quickly (Stamps, 2006) and it may take time for individuals to gain personal information (Doligez *et al.*, 2002). This could result in a delay between when birds initially arrive at a location and settle at a final breeding site.

Secondly, it is likely that some portion of the shifting distribution dynamics could be due to behavioural thermoregulation (Bernardo, 2014). Mammals (Long *et al.*, 2014) and birds (Dolby & Grubb, 1999) have both been shown to alter their behaviour in response to temperature conditions. Karr & Freemark (1983) hypothesized that tropical birds often avoided extremely wet or dry sites (depending on time of year) for physiological reasons rather than due to food resources. Other studies have documented upward shifts along elevational gradients (e.g., Klemp, 2003), which are suggested to indicate shifts towards climatically favourable sites amid seasonal warming. Shifts in distributions towards more thermally appropriate sites could also occur at finer, within-territory scales.

Finally, within-season movement may enable birds to capitalize on ephemeral resources available in spatially distinct locations either within territory boundaries or at broader scales (Diggs *et al.*, 2011). Within-season shifting could represent upgrading along ecological gradients in habitat quality to track changes in resources. Hence, motivation behind settlement, vacancy and within-territory habitat use decisions could potentially be linked to temperature-sensitive food resources – particularly arthropod abundance (Lack, 1954; Martin, 1987; Rodenhouse *et al.*, 2003). Temperature and degree days in late winter and spring are known to be strongly associated with important phenological events such as bud break (Yu *et al.*, 2010), insect emergence (Both *et al.*, 2009) and insect abundance (Kingsolver *et al.*, 2011).

It is important to note that we did not measure movement directly through methods such as telemetry (e.g., Gow & Stutchbury, 2013). In particular, we were only able to quantify distributional changes within a season based on modelled 'colonization' and 'extinction' rates (MacKenzie *et al.*, 2006). Despite the fact that our models were designed to account for imperfect detection, within-territory movements of birds into and outside of our count circle between sampling sessions could result in the settlement and vacancy patterns that we observed (Betts *et al.*, 2008). However, based on simulation studies performed by Chandler *et al.* (2011), temporary emigration from a sample location is only likely to bias parameters estimates when it is not random. Further, we did not find strong support for a home-range size effect on colonization and extinction rates (Appendix S3). However, from the most conservative standpoint, estimated rates of vacancy and settlement could also be due to within-territory shifts in resource use, or gradients in density associated with microclimate.

Implications

We have provided evidence that high-resolution temperature data are useful for species distribution modelling. Although the logistics of obtaining such data may be challenging (Bennie *et al.*, 2014), we argue that failing to incorporate local microclimate variability masks important occupancy processes. The unexpectedly high relative importance of site-level climate over local vegetation in local habitat selection versus regional scales could stem from mismatches in data quality across scales; climate data tend to be measured well at broad scales, but not fine scales. In contrast, vegetation data are often collected at high resolution (and accuracy) at fine scales, but not broad scales (Betts *et al.*, 2006). Our results indicate that lack of fine-scale temperature data may mask the relative role of temperature and could lead to the appearance of vegetation as the key driver of distributions at fine scales (Luoto *et al.*, 2007). For some temperature metrics, widely available elevation and aspect data could serve as surrogates for fine-scale temperature; however, results from Frey *et al.* (2016) indicate that vegetation structure and microtopography also have important implications for under-canopy temperature.

While most species showed apparent habitat shifts in response to site temperature conditions, the direction of these responses varied by species. Moritz & Agudo (2013) also found that many species had highly variable responses to climate. Many range-shift studies have reported high variability in both the degree and direction of range shifts (Lenoir *et al.*, 2010; Chen *et al.*, 2011). Microclimate heterogeneity and species-specific responses to local-scale temperature could explain the inconsistencies between predicted and observed responses to climate change (Buckley & Kingsolver, 2012).

Our results showing within-season distribution dynamics for most species we examined suggest that forest bird species potentially have the behavioural flexibility to track favourable microclimates within a season (Boyles *et al.*, 2011; Tuomainen & Candolin, 2011). In montane landscapes, complex terrain could create buffered 'microrefugia' (Dobrowski, 2010). Microclimate heterogeneity may be an important factor in providing options for behavioural adaptation (Bonebrake *et al.*, 2014) in the face of regional climate changes. Stable populations in heterogeneous landscapes could stem from increased options for tracking microclimate (Oliver *et al.*, 2010). Indeed, we found some evidence for population declines in species we identified as being 'cool-associated' (mean trend [95% CIs] = −1.06%/year [−1.96 to −0.16]) at the regional scale (Breeding Bird Survey 2002–2012 trends from the Pacific Northwest temperate rainforest region) relative to their warm-associated counterparts (−0.16%/year [−0.99 to 0.68], see Appendix S7). This suggests that at least regionally, buffering capacity may be insufficient to sustain stable populations for cool-associated species in the face of climate change.

Conclusions

Our results show that distributional patterns of forest birds are strongly associated with fine-scale thermal regimes in mountainous landscapes. Birds tended to both vacate and settle sites with particular microclimate conditions, even after accounting for the influence of vegetation and imperfect detection. This behavioural flexibility to adapt to changes within a breeding season appears widespread as it was demonstrated by almost all members of the forest bird community we examined. Future efforts should examine the degree to which such vagility and apparent flexibility in habitat selection might propagate to buffer such species against the impact of long-term climate change.

ACKNOWLEDGEMENTS

This research was possible with support from multiple grants and awards: an NSF-IGERT fellowship (NSF-0333257), a Department of the Interior Northwest Climate Science Center graduate fellowship and an Andrews Forest LTER graduate research assistantship (NSF DEB-0823380) all awarded to S.J.K.F. Research and support were provided by the H. J. Andrews Experimental Forest research program, funded by the National Science Foundation's Long-Term Ecological Research Program (NSF DEB-0823380), US Forest Service Pacific Northwest Research Station and Oregon State University. The project described in this publication was also supported by a grant to M.G.B. from the Department of the Interior through Cooperative Agreement No. G11AC20255 from the US Geological Survey and a National Science Foundation grant awarded to M.G.B. (NSF ARC-0941748). The contents of this manuscript are solely the responsibility of the authors and do not represent the views of the Northwest Climate Science Center, the USGS or the USFS. We extend a special thanks to Jay Sexton for providing logistical field support. Finally, this work would not have been possible without our exceptional field assistants (Evan Jackson, April Bartelt, Sean Ashe, Sveta Yegorova, Andrea Mott and Katelin Stanley).

REFERENCES

Araújo, M.B. & Pearson, R.G. (2005) Equilibrium of species' distributions with climate. *Ecography*, **28**, 693–695.

Araújo, M.B., Thuiller, W., Williams, P.H. & Reginster, I. (2005) Downscaling European species atlas distributions to a finer resolution: implications for conservation planning. *Global Ecology and Biogeography*, **14**, 17–30.

Bennie, J., Wilson, R.J., Maclean, I.M.D. & Suggitt, A.J. (2014) Seeing the woods for the trees – when is microclimate important in species distribution models? *Global Change Biology*, **20**, 2699–2700.

Bernardo, J. (2014) Biologically grounded predictions of species resistance and resilience to climate change. *Proceedings of the National Academy of Sciences USA*, **111**, 5450–5451.

Betts, M.G., Diamond, A.W., Forbes, G.J., Villard, M.A. & Gunn, J.S. (2006) The importance of spatial autocorrelation, extent and resolution in predicting forest bird occurrence. *Ecological Modelling*, **191**, 197–224.

Betts, M.G., Rodenhouse, N.L., Sillett, T.S., Doran, P.J. & Holmes, R.T. (2008) Dynamic occupancy models reveal within-breeding season movement up a habitat quality gradient by a migratory songbird. *Ecography*, **31**, 592–600.

Beyer, H.L. (2004) Hawth's Analysis Tools for ArcGIS. http://www.spatialecology.com/htools (accessed 1 May 2009).

Bonebrake, T.C., Boggs, C.L., Stamberger, J.A., Deutsch, C.A. & Ehrlich, P.R. (2014) From global change to a butterfly flapping: biophysics and behaviour affect tropical climate change impacts. *Proceedings of the Royal Society B: Biological Sciences*, **281**, 20141264.

Both, C. & Visser, M.E. (2005) The effect of climate change on the correlation between avian life-history traits. *Global Change Biology*, **11**, 1606–1613.

Both, C., Bijlsma, R.G. & Visser, M.E. (2005) Climatic effects on timing of spring migration and breeding in a long-distance migrant, the pied flycatcher *Ficedula hypoleuca*. *Journal of Avian Biology*, **36**, 368–373.

Both, C., Bouwhuis, S., Lessells, C.M. & Visser, M.E. (2006) Climate change and population declines in a long-distance migratory bird. *Nature*, **441**, 81–83.

Both, C., van Asch, M., Bijlsma, R.G., van den Burg, A.B. & Visser, M.E. (2009) Climate change and unequal phenological changes across four trophic levels: constraints or adaptations? *Journal of Animal Ecology*, **78**, 73–83.

Boucher-Lalonde, V., Morin, A. & Currie, D.J. (2014) A consistent occupancy–climate relationship across birds and mammals of the Americas. *Oikos*, **123**, 1029–1036.

Boyles, J.G., Seebacher, F., Smit, B. & McKechnie, A.E. (2011) Adaptive thermoregulation in endotherms may alter responses to climate change. *Integrative and Comparative Biology*, **51**, 676–690.

Brambilla, M. & Rubolini, D. (2009) Intra-seasonal changes in distribution and habitat associations of a multi-brooded bird species: implications for conservation planning. *Animal Conservation*, **12**, 71–77.

Brown, J.H. (1995) *Macroecology*. University of Chicago Press, Chicago, IL.

Buckley, L.B. & Kingsolver, J.G. (2012) Functional and phylogenetic approaches to forecasting species' responses to climate change. *Annual Review of Ecology, Evolution, and Systematics*, **43**, 205–226.

Burnham, K.P. & Anderson, D.R. (2002) *Model Selection and Multimodel Inference: A Practical Information-Theoretic Approach*, 2nd edn. Springer-Verlag Inc, New York, NY.

Cade, B.S. (2015) Model averaging and muddled multimodel inferences. *Ecology*, **96**, 2370–2382.

Chandler, R.B. & King, D.I. (2011) Habitat quality and habitat selection of golden-winged warblers in Costa Rica: an application of hierarchical models for open populations. *Journal of Applied Ecology*, **48**, 1038–1047.

Chandler, R.B., Royle, J.A. & King, D.I. (2011) Inference about density and temporary emigration in unmarked populations. *Ecology*, **92**, 1429–1435.

Chen, I.C., Hill, J.K., Ohlemuller, R., Roy, D.B. & Thomas, C.D. (2011) Rapid range shifts of species associated with high levels of climate warming. *Science*, **333**, 1024–1026.

Cumming, S.G., Stralberg, D., Lefevre, K.L., Sólymos, P., Bayne, E.M., Fang, S., Fontaine, T., Mazerolle, D., Schmiegelow, F.K.A. & Song, S.J. (2014) Climate and vegetation hierarchically structure patterns of songbird distribution in the Canadian boreal region. *Ecography*, **37**, 137–151.

Devictor, V., Julliard, R., Couvet, D. & Jiguet, F. (2008) Birds are tracking climate warming, but not fast enough. *Proceedings of the Royal Society B: Biological Sciences*, **275**, 2743–2748.

Diggs, N.E., Marra, P.P. & Cooper, R.J. (2011) Resource limitation drives patterns of habitat occupancy during the nonbreeding season for an omnivorous songbird. *Condor*, **113**, 646–654.

Dobrowski, S.Z. (2010) A climatic basis for microrefugia: the influence of terrain on climate. *Global Change Biology*, **17**, 1022–1035.

Dolby, A.S. & Grubb, T.C. (1999) Effects of winter weather on horizontal and vertical use of isolated forest fragments by bark-foraging birds. *Condor*, **101**, 408–412.

Doligez, B., Danchin, E. & Clobert, J. (2002) Public information and breeding habitat selection in a wild bird population. *Science*, **297**, 1168–1170.

Ellis, T.M. & Betts, M.G. (2011) Bird abundance and diversity across a hardwood gradient within early seral plantation forest. *Forest Ecology and Management*, **261**, 1372–1381.

ESRI (2011) *ArcGIS Desktop: Release 10*. Environmental Systems Research Institute, Redlands, CA.

Fiske, I. & Chandler, R. (2011) unmarked: An R package for fitting hierarchical models of wildlife occurrence and abundance. *Journal of Statistical Software*, **43**, 1–23.

Franklin, J., Davis, F.W., Ikegami, M., Syphard, A.D., Flint, L.E., Flint, A.L. & Hannah, L. (2013) Modeling plant species distributions under future climates: how fine scale do climate projections need to be? *Global Change Biology*, **19**, 473–483.

Fretwell, S.D. & Lucas, H.L. (1969) On territorial behavior and other factors influencing habitat distribution in birds. *Acta Biotheoretica*, **19**, 16–36.

Frey, S.J.K., Hadley, A.S., Johnson, S.L., Schulze, M., Jones, J.A. & Betts, M.G. (2016) Spatial models reveal microclimatic buffering capacity of old-growth forests. *Science Advances*, **2**, e1501392.

Fu, Y.H., Campioli, M., Deckmyn, G. & Janssens, I.A. (2012) The impact of winter and spring temperatures on temperate tree budburst dates: results from an experimental climate manipulation. *PLoS One*, **7**, e47324.

Gilroy, J.J., Anderson, G.Q.A., Grice, P.V., Vickery, J.A. & Sutherland, W.J. (2010) Mid-season shifts in the habitat associations of Yellow Wagtails *Motacilla flava* breeding in arable farmland. *Ibis*, **152**, 90–104.

Gow, E.A. & Stutchbury, B.J.M. (2013) Within-season nesting dispersal and molt dispersal are linked to habitat shifts in a Neotropical migratory songbird. *Wilson Journal of Ornithology*, **125**, 696–708.

Gutiérrez Illán, J., Thomas, C.D., Jones, J.A., Wong, W.-K., Shirley, S.M. & Betts, M.G. (2014) Precipitation and winter temperature predict long-term range-scale abundance changes in Western North American birds. *Global Change Biology*, **20**, 3351–3364.

Hagar, J.C. (2007) Wildlife species associated with non-coniferous vegetation in Pacific Northwest conifer forests: a review. *Forest Ecology and Management*, **246**, 108–122.

Hildén, O. (1965) Habitat selection in birds: a review. *Annales Zoologici Fennici*, **2**, 53–75.

Hitch, A.T. & Leberg, P.L. (2007) Breeding distributions of North American bird species moving north as a result of climate change. *Conservation Biology*, **21**, 534–539.

Hoover, J.P. (2003) Decision rules for site fidelity in a migratory bird, the prothonotary warbler. *Ecology*, **84**, 416–430.

Hosmer, D.W., Hosmer, T., Le Cessie, S. & Lemeshow, S. (1997) A comparison of goodness-of-fit tests for the logistic regression model. *Statistics in Medicine*, **16**, 965–980.

Hosmer, D.W., Jr, Lemeshow, S. & Sturdivant, R.X. (2013) *Applied Logistic Regression*, 3rd edn. John Wiley & Sons, Inc., Hoboken, New Jersey.

Huey, R.B., Kearney, M.R., Krockenberger, A., Holtum, J.A.M., Jess, M. & Williams, S.E. (2012) Predicting organismal vulnerability to climate warming: roles of behaviour, physiology and adaptation. *Philosophical Transactions of the Royal Society B-Biological Sciences*, **367**, 1665–1679.

IPCC (2014) *Climate Change 2014: Impacts, Adaptation, and Vulnerability. Part A: Global and Sectoral Aspects. Contribution of Working Group II to the Fifth Assessment Report of the Intergovernmental Panel on Climate Change*. p. 1132, Cambridge University Press, Cambridge, UK and New York, NY, USA.

Karr, J.R. & Freemark, K.E. (1983) Habitat selection and environmental gradients: dynamics in the "stable" tropics. *Ecology*, **64**, 1481–1494.

Kearney, M., Shine, R. & Porter, W.P. (2009) The potential for behavioral thermoregulation to buffer "cold-blooded" animals against climate warming. *Proceedings of the National Academy of Sciences USA*, **106**, 3835–3840.

Keppel, G., Van Niel, K.P., Wardell-Johnson, G.W., Yates, C.J., Byrne, M., Mucina, L., Schut, A.G.T., Hopper, S.D. & Franklin, S.E. (2012) Refugia: identifying and understanding safe havens for biodiversity under climate change. *Global Ecology and Biogeography*, **21**, 393–404.

Kéry, M. & Chandler, R. (2012) *Unmarked Vignette: Dynamic Occupancy Models in Unmarked*. Swiss Ornithological Institute and USGS Patuxent Wildlife Research Center, Sempach, Switzerland and Maryland, USA.

Kingsolver, J.G., Woods, H.A., Buckley, L.B., Potter, K.A., MacLean, H.J. & Higgins, J.K. (2011) Complex life cycles and the responses of insects to climate change. *Integrative and Comparative Biology*, **51**, 719–732.

Klemp, S. (2003) Altitudinal dispersal within the breeding season in the Grey Wagtail *Motacilla cinerea*. *Ibis*, **145**, 509–511.

Lack, D. (1954) *The Natural Regulation of Animal Numbers*. Oxford University Press, London.

Legendre, P. (1993) Spatial autocorrelation: Trouble or new paradigm. *Ecology*, **74**, 1659–1673.

Lenoir, J., Gegout, J.C., Guisan, A., Vittoz, P., Wohlgemuth, T., Zimmermann, N.E., Dullinger, S., Pauli, H., Willner, W. & Svenning, J.C. (2010) Going against the flow: potential mechanisms for unexpected downslope range shifts in a warming climate. *Ecography*, **33**, 295–303.

Lichstein, J.W., Simons, T.R., Shriner, S.A. & Franzreb, K.E. (2002) Spatial autocorrelation and autoregressive models in ecology. *Ecological Monographs*, **72**, 445–463.

Logan, M.L., Huynh, R.K., Precious, R.A. & Calsbeek, R.G. (2013) The impact of climate change measured at relevant spatial scales: new hope for tropical lizards. *Global Change Biology*, **19**, 3093–3102.

Long, R.A., Bowyer, R.T., Porter, W.P., Mathewson, P., Monteith, K.L. & Kie, J.G. (2014) Behavior and nutritional condition buffer a large-bodied endotherm against direct and indirect effects of climate. *Ecological Monographs*, **84**, 513–532.

Lumpkin, H.A. & Pearson, S.M. (2013) Effects of exurban development and temperature on bird species in the southern Appalachians. *Conservation Biology*, **27**, 1069–1078.

Luoto, M., Virkkala, R. & Heikkinen, R.K. (2007) The role of land cover in bioclimatic models depends on spatial resolution. *Global Ecology and Biogeography*, **16**, 34–42.

MacArthur, R.H., MacArthur, J.W. & Preer, J. (1962) On bird species diversity II: prediction of bird census from habitat measurements. *The American Naturalist*, **96**, 167–174.

MacKenzie, D.I. & Bailey, L.L. (2004) Assessing the fit of site-occupancy models. *Journal of Agricultural, Biological & Environmental Statistics*, **9**, 300–318.

MacKenzie, D., Nichols, J., Hines, J., Knutson, M. & Franklin, A. (2003) Estimating site occupancy, colonization, and local extinction when a species is detected imperfectly. *Ecology*, **84**, 2200–2207.

MacKenzie, D., Nichols, J., Royle, J., Pollock, K., Bailey, L. & Hines, J. (2006) *Occupancy Estimation and Modeling: Inferring Patterns and Dynamics of Species Occurrence*. Elsevier Inc., Oxford, UK.

Maggini, R., Lehmann, A., Kéry, M., Schmid, H., Beniston, M., Jenni, L. & Zbinden, N. (2011) Are Swiss birds tracking climate change?: Detecting elevational shifts using response curve shapes. *Ecological Modelling*, **222**, 21–32.

Martin, T.E. (1987) Food as a limit on breeding birds - a life-history perspective. *Annual Review of Ecology and Systematics*, **18**, 453–487.

McClure, C.J.W. & Hill, G.E. (2012) Dynamic versus static occupancy: how stable are habitat associations through a breeding season? *Ecosphere*, **3**, 60. http://dx.doi.org/10.1890/ES12-00034.1

Mitikka, V., Heikkinen, R.K., Luoto, M., Araujo, M.B., Saarinen, K., Poyry, J. & Fronzek, S. (2008) Predicting range expansion of the map butterfly in Northern Europe using bioclimatic models. *Biodiversity and Conservation*, **17**, 623–641.

Moritz, C. & Agudo, R. (2013) The future of species under climate change: Resilience or decline? *Science*, **341**, 504–508.

Oliver, T., Roy, D.B., Hill, J.K., Brereton, T. & Thomas, C.D. (2010) Heterogeneous landscapes promote population stability. *Ecology Letters*, **13**, 473–484.

Parmesan, C. & Yohe, G. (2003) A globally coherent fingerprint of climate change impacts across natural systems. *Nature*, **421**, 37–42.

Patsiou, T.S., Conti, E., Zimmermann, N.E., Theodoridis, S. & Randin, C.F. (2013) Topo-climatic microrefugia explain the persistence of a rare endemic plant in the Alps during the last 21 millennia. *Global Change Biology*, **20**, 2286–2300.

Pearson, R.G. & Dawson, T.P. (2003) Predicting the impacts of climate change on the distribution of species: are bioclimate envelope models useful? *Global Ecology & Biogeography*, **12**, 361–371.

Peterson, A.T., Ortega-Huerta, M.A., Bartley, J., Sanchez-Cordero, V., Soberon, J., Buddemeier, R.H. & Stockwell, D.R.B. (2002) Future projections for Mexican faunas under global climate change scenarios. *Nature*, **416**, 626–629.

Poole, A., Editor (2005) *The Birds of North America Online*. Cornell Laboratory of Ornithology, Ithaca, NY. http://bna.birds.cornell.edu/BNA/.

Potter, K.A., Woods, H.A. & Pincebourde, S. (2013) Microclimatic challenges in global change biology. *Global Change Biology*, **19**, 2932–2939.

Pulliam, H.R. & Danielson, B.J. (1991) Sources, sinks, and habitat selection: a landscape perspective on population-dynamics. *The American Naturalist*, **137**, S50–S66.

R Development Core Team (2011) *R: A Language and Environment for Statistical Computing*. R Foundation for Statistical Computing, Vienna, Austria.

Ritchie, L.E., Betts, M.G., Forbes, G. & Vernes, K. (2009) Effects of landscape composition and configuration on northern flying squirrels in a forest mosaic. *Forest Ecology and Management*, **257**, 1920–1929.

Rodenhouse, N.L., Sillett, T.S., Doran, P.J. & Holmes, R.T. (2003) Multiple density-dependence mechanisms regulate a migratory bird population during the breeding season. *Proceedings of the Royal Society B: Biological Sciences*, **270**, 2105–2110.

Root, T. (1988) Environmental factors associated with avian distributional boundaries. *Journal of Biogeography*, **15**, 489–505.

Rota, C.T., Fletcher, R.J. Jr, Dorazio, R.M. & Betts, M.G. (2009) Occupancy estimation and the closure assumption. *Journal of Applied Ecology*, **46**, 1173–1181.

Scheffers, B.R., Edwards, D.P., Diesmos, A., Williams, S.E. & Evans, T.A. (2014) Microhabitats reduce animal's exposure to climate extremes. *Global Change Biology*, **20**, 495–503.

Scherrer, D., Schmid, S. & Korner, C. (2011) Elevational species shifts in a warmer climate are overestimated when based on weather station data. *International Journal of Biometeorology*, **55**, 645–654.

Seavy, N.E., Viers, J.H. & Wood, J.K. (2009) Riparian bird response to vegetation structure: a multiscale analysis using LiDAR measurements of canopy height. *Ecological Applications*, **19**, 1848–1857.

Sheldon, K.S., Yang, S. & Tewksbury, J.J. (2011) Climate change and community disassembly: impacts of warming on tropical and temperate montane community structure. *Ecology Letters*, **14**, 1191–1200.

Stamps, J.A. (2006) The silver spoon effect and habitat selection by natal dispersers. *Ecology Letters*, **9**, 1179–1185.

Storlie, C., Merino-Viteri, A., Phillips, B., VanDerWal, J., Welbergen, J. & Williams, S. (2014) Stepping inside the niche: microclimate data are critical for accurate assessment of species' vulnerability to climate change. *Biology Letters*, **10**, 20140576.

Stralberg, D., Jongsomjit, D., Howell, C.A., Snyder, M.A., Alexander, J.D., Wiens, J.A. & Root, T.L. (2009) Re-shuffling of species with climate disruption: a no-analog future for California birds? *PLoS One*, **4**, e6825.

Switzer, P.V. (1997) Factors affecting site fidelity in a territorial animal, *Perithemis tenera*. *Animal Behaviour*, **53**, 865–877.

Thomas, C.D. (2010) Climate, climate change and range boundaries. *Diversity and Distributions*, **16**, 488–495.

Thomas, C.D., Cameron, A., Green, R.E., Bakkenes, M., Beaumont, L.J., Collingham, Y.C., Erasmus, B.F.N., de Siqueira, M.F., Grainger, A., Hannah, L., Hughes, L., Huntley, B., van Jaarsveld, A.S., Midgley, G.F., Miles, L., Ortega-Huerta, M.A., Townsend Peterson, A., Phillips, O.L. & Williams, S.E. (2004) Extinction risk from climate change. *Nature*, **427**, 145–148.

Thuiller, W., Araujo, M.B. & Lavorel, S. (2004a) Do we need land-cover data to model species distributions in Europe? *Journal of Biogeography*, **31**, 353–361.

Thuiller, W., Araujo, M.B., Pearson, R.G., Whittaker, R.J., Brotons, L. & Lavorel, S. (2004b) Biodiversity conservation: uncertainty in predictions of extinction risk. *Nature*, **430**, 34.

Tingley, M.W. & Beissinger, S.R. (2009) Detecting range shifts from historical species occurrences: new perspectives on old data. *Trends in Ecology and Evolution*, **24**, 625–633.

Tingley, M.W., Koo, M.S., Moritz, C., Rush, A.C. & Beissinger, S.R. (2012) The push and pull of climate change causes heterogeneous shifts in avian elevational ranges. *Global Change Biology*, **18**, 3279–3290.

Tuomainen, U. & Candolin, U. (2011) Behavioural responses to human-induced environmental change. *Biological Reviews*, **86**, 640–657.

Vatka, E., Orell, M. & Rytkönen, S. (2011) Warming climate advances breeding and improves synchrony of food demand and food availability in a boreal passerine. *Global Change Biology*, **17**, 3002–3009.

Virkkala, R., Heikkinen, R.K., Leikola, N. & Luoto, M. (2008) Projected large-scale range reductions of northern-boreal land bird species due to climate change. *Biological Conservation*, **141**, 1343–1353.

Virkkala, R., Heikkinen, R.K., Lehikoinen, A. & Valkama, J. (2014) Matching trends between recent distributional changes of northern-boreal birds and species-climate model predictions. *Biological Conservation*, **172**, 124–127.

Yu, H., Luedeling, E. & Xu, J. (2010) Winter and spring warming result in delayed spring phenology on the Tibetan Plateau. *Proceedings of the National Academy of Sciences USA*, **107**, 22151–22156.

SUPPORTING INFORMATION

Additional Supporting Information may be found in the online version of this article:

Appendix S1 Details concerning placement of HOBO temperature sensors and processing of temperature data.

Appendix S2 Details concerning LiDAR-derived variables for vegetation structure and principal component analysis.

Appendix S3 Dynamic occupancy model structure and additional details.

Appendix S4 Methods for creating spatial maps of bird distributions as a function of microclimate and vegetation structure variables.

Appendix S5 Results from home range tests on assumptions of dynamic occupancy models.

Appendix S6 Dryad digital depository for AIC model selection tables.

Appendix S7 Methods for Breeding Bird Survey population trends comparison between cool- and warm-associated species.

Figure S1 Bi-plot of the first two components (PC1 on the *x*-axis and PC2 on the *y*-axis) from the principal component analysis showing how vegetation structure metrics differ between old-growth/mature forest sites (blue dots) and plantations (red dots).

Figure S2 Maps of study area showing sample points, elevational gradient, and canopy height.

Figure S3 Predicted occupancy probability maps for cool-associated species.

Figure S4 Predicted occupancy probability maps for warm-associated species.

Table S1 LiDAR-derived vegetation structure variables used in the principal component analysis.

Table S2 Results from the principal component analysis of all vegetation structure predictor variables.

Table S3 Deciduous tree and large shrub species used to quantify forest composition at our sample points.

Table S4 Pearson's correlation coefficients between all predictor variables.

Table S5 Coefficients (Est) and standard errors (SE) for initial occupancy (ψ).

Table S6 Coefficients (Est) and standard errors (SE) for detection probability (*p*) as a function of survey covariates.

Table S7 Coefficients (Est) and standard errors (SE) for detection probability (*p*) as a function of environmental covariates.

Table S8 Coefficients (Est) and standard errors (SE) for all parameters from constant models.

Table S9 Comparison of effect sizes between fine-scale temperature and vegetation on settlement and vacancy.

Table S10 Goodness-of-fit bootstrap results for top models.

Table S11 Results from tests for spatial autocorrelation in the residuals from the top models.

Table S12 Interactions between temperature and vegetation variables from the top models for occupancy, colonization and extinction.

BIOSKETCHES

Sarah J. K. Frey, Adam S. Hadley and Matthew G. Betts are based in the Forest Biodiversity Research Network in the Department of Forest Ecosystems and Society at Oregon State University (http://www.fsl.orst.edu/flel/index.htm). They are members of a research team directed at understanding climatic and land-use factors underlying the spatial and temporal distribution of biodiversity in forests of the Americas.

Author contributions: All authors conceived the ideas and collected the data; S.J.K.F analysed the data; and all authors wrote the manuscript.

Editor: Mark Robertson

SUPPORTING INFORMATION

Microclimate predicts within-season distribution dynamics of montane forest birds

Sarah J. K. Frey[1*], Adam S. Hadley[1,2], Matthew G. Betts[1]

[1]Forest Biodiversity Research Network, Department of Forest Ecosystems & Society, Oregon State University, Corvallis, OR 97331, USA

[2]Department of Ecology & Evolutionary Biology, University of Toronto, Mississauga, ON L5L 1C6, Canada

**Corresponding author: sarah.frey@oregonstate.edu*

Appendix S1. Details concerning placement of HOBO temperature sensors and processing of temperature data.

Deployment and maintenance of temperature sensors

All HOBOs were placed 1.5m from the ground near the center of the sample point location. Loggers were often placed ~1-2m downhill from a tree when possible to reduce the chances of being buried by snow in steep locations. We used a flexible fiberglass post to support the logger and to allow for bending of the entire unit under the weight of snow. We used half of a 3-inch diameter schedule 40 PVC pipe, cut to 6-in in length for a sun shield. We oriented all temperature loggers to face south using a compass. We programed temperature to be recorded every 20 minutes. We downloaded data from the units twice a year (May and July) and changed the batteries once a year based on sampling frequency (generally on the second offload session of each year).

Logger details, calibration and data cleaning

At the majority of the sites (n=167) we used HOBO pendant data loggers (Onset HOBO Pendant Temperature/Light Data Logger 64K, model UA-002-64 [Fig. S7]). At 16 sites we employed HOBO water temperature data loggers (Onset HOBO Water Temperature Pro v2 Data Logger, model U22-001). All units were calibrated by submersion in both hot (20.3°C) and cold (with ice, 0°C) water prior to deployment. Occasional malfunctioning units and seasonal snow cover created gaps in our dataset. Additionally, extreme anomalous values were occasionally produced by the units. We processed the data as described in the following section (Temperature data processing) before all statistical analysis.

Temperature data processing

We first compiled offloaded files into a continuous time series by site. We used a Python script (http://www.python.org) to flag, clean, average, and fill datasets. Flagging identified several problems including no data, incorrect logging intervals, extreme values, jumps in values, and periods when the logger was under snow. Data for which the logger had recorded date and time but no temperature were flagged as no data. Incorrect logging intervals (i.e., those not separated by the programmed interval of 15 or 20 minutes) were commonly associated with missing values and were flagged for easy identification. Values outside of the sensor range (-20° to 70°C) were flagged as extreme. Jumps in values were defined as a change in temperature of >5°C in one time interval and appeared to be related to infrequent faulty readings. Our method for flagging snow cover used a forward 'rolling window' approach. If the variation in temperatures within a 24-hr period was <0.5°C and the temperatures <1°C, we considered that time period to indicate that snow covered the data logger. To account for the forward rolling window, we also flagged periods in which snow was present in the past 24-hrs.

Appendix S2. Details concerning LiDAR-derived variables for vegetation structure and principal component analysis.

Variables derived from the Light Detection And Ranging (LiDAR) dataset included: 1) Canopy height (CH), 2) % cover mid-canopy (2-10m) and upper canopy (>10m), 3) Biomass, 4) Coefficient of variation in canopy height, 5) Height of median return (HOME) and 6) Vertical distribution ratio (VDR). HOME describes the height at which the bulk of the canopy exists (***53***). VDR is an index of vertical distribution of intercepted canopy components (***53***). It is calculated as follows: [CH – HOME]/CH. Lower VDR values represent a shorter distance between CH and HOME, indicating a larger understory canopy component (***53***).

To quantify the gradient in forest structure and integrate vegetation structure variables into a reduced number of components, we used the first two principal components (PC) from a principal component analysis (PCA) of all our LiDAR-derived vegetation variables at the 25-m scale (13 variables, see Table S1). PC1 and 2 explained 75% of the variation present in the forest structure metrics and appeared to effectively differentiate between plantations and older forests. PC1 explained 45% of variance in vegetation structure and increasing values were associated with old-growth forest characteristics. PC2 explained 30% of variation in vegetation structure and higher values tended to be more associated with forest plantations. These gradients represent the predominant forest types on Federal land in the region (Spies *et al.*, 2007). Sites with low PC1 values had less biomass (mean and SD), lower canopies (mean and SD), and less cover 2-10m and >10m (Table S2). The individual LiDAR metrics effectively distinguished between plantation and old growth/mature forest sites; a discriminant function analysis (Fisher, 1936) showed that prediction accuracy was 85.3% for plantation sites and 90.4% for old-growth/mature forest sites. Further, our LiDAR metrics were congruent with previously reported structural differences between old-growth and secondary Douglas-fir forest in the Pacific Northwest (Franklin *et al.*, 2002).

Table S1. LiDAR-derived vegetation structure variables used in the principal component analysis.

Variable name	Description
Mean canopy height	Mean LiDAR vegetation height (m)
Mean biomass	Mean biomass, derived from LiDAR vegetation dataset
Mean cover 0-2m	Mean canopy point density of points 0-2m off the ground (all vegetation LiDAR returns)
Mean cover 2-10m	Mean canopy point density of points 0-2m off the ground (all vegetation LiDAR returns)
Mean cover >10m	Mean canopy point density of points 0-2m off the ground (all vegetation LiDAR returns)
Mean coef of variation	Mean height metric from first returns only, coefficient of variation exclude points below 1 meter, vegetation LiDAR
Mean HOME	Mean height of median energy (HOME, m), HOME is the height at which 50% of energy returned
Mean VDR	Mean vertical distribution ratio (VDR, unit-less), Calculated as (canopy height – HOME)/canopy height. VDR can be defined as “a normalized ratio between the canopy height and HOME products, which provided an index of the vertical distribution of intercepted canopy elements (Goetz et al. 2010).
SD canopy height	Mean canopy height (m), vegetation LiDAR
SD biomass	Standard deviation of biomass (Mg/ha), derived from LiDAR vegetation dataset
SD cover 0-2m	Standard deviation of canopy point density of points 0-2m off the ground (all vegetation LiDAR returns)
SD cover 2-10m	Standard deviation of canopy point density of points 2-10m off the ground (all vegetation LiDAR returns)
SD cover >10m	Standard deviation of canopy point density of points >10m off the ground (all vegetation LiDAR returns)

Table S2. Results from the principal component analysis of all vegetation structure predictor variables. See Table S1 for a complete list of predictor variables. (**A**) Standard deviation and proportion of variance for the first eight out of 11 principal components. (**B**) Contributions of individual vegetation structure variables for the first eight principal components.

A	PC1	PC2	PC3	PC4	PC5	PC6	PC7	PC8
Standard deviation	2.22	1.82	1.02	0.88	0.76	0.39	0.37	0.22
Proportion of Variance	0.45	0.30	0.09	0.07	0.05	0.01	0.01	0.00
Cumulative Proportion	0.45	0.75	0.84	0.91	0.96	0.98	0.99	1.00

B	PC1	PC2	PC3	PC4	PC5	PC6	PC7	PC8
Mn biomass	0.41	-0.19	0.08	-0.14	0.11	-0.11	-0.37	0.30
SD biomass	0.33	-0.34	0.06	0.00	0.07	-0.61	0.34	-0.17
Mn can ht	0.44	0.02	0.07	-0.05	0.01	0.19	-0.24	0.17
SD can ht	0.32	-0.37	-0.01	-0.07	-0.13	-0.05	0.22	-0.22
Mn cover >10m	0.36	0.26	0.07	0.14	-0.26	0.36	0.67	0.29
SD cover >10m	-0.11	-0.38	-0.07	0.23	-0.83	0.03	-0.23	0.06
Mn cover 2-10m	-0.11	-0.20	0.65	0.65	0.23	0.01	-0.02	0.17
SD cover 2-10m	0.14	-0.09	-0.71	0.62	0.26	0.07	-0.04	-0.02
HOME	0.44	0.08	0.05	-0.02	0.01	0.16	-0.32	0.05
CV can ht	-0.03	-0.51	0.08	-0.17	0.22	0.64	0.08	-0.38
VDR	-0.24	-0.42	-0.20	-0.25	0.16	0.03	0.17	0.74

Figure S1. Bi-plot of the first two components (PC1 on the x-axis and PC2 on the y-axis) from the principal component analysis showing how vegetation structure metrics differ between old-growth/mature forest sites (blue dots) and plantations (red dots). The ellipses represent the 68% normal data of the distribution of points in each category (plantation and mature/old growth).

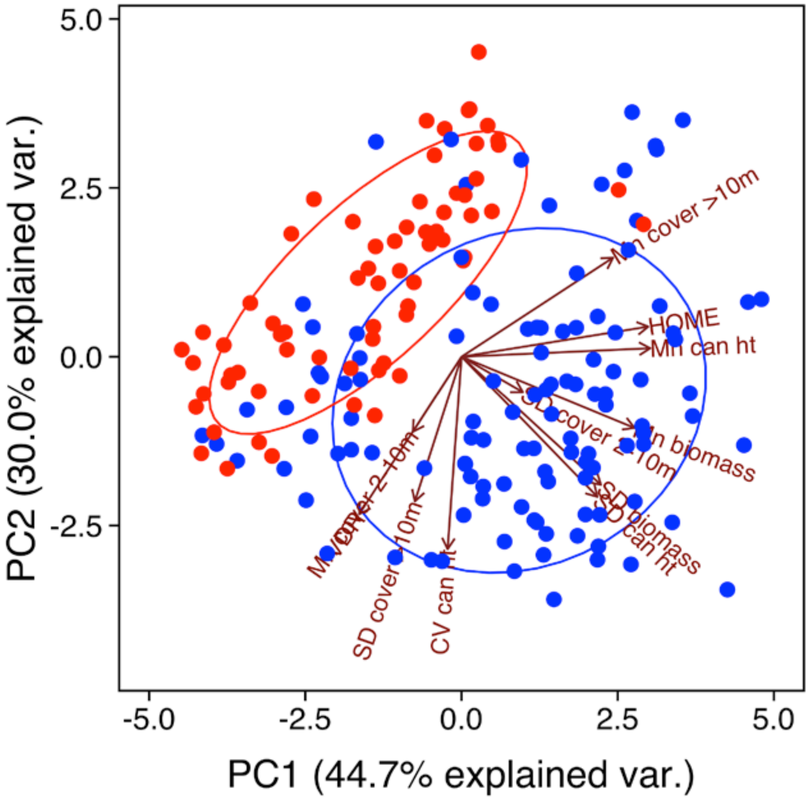

Appendix S3. Dynamic occupancy model structure and additional details.

Dynamic occupancy models assume that populations are closed between *j* sub-counts and movement is explicitly modeled between *t* sampling occasions by the dynamic parameters (γ and ε). This is a Markovian process in that occupancy in time *t* is dependent on occupancy in time $t - 1$. A site can go from unoccupied in time $t - 1$ to occupied in time *t* (settlement event) or from occupied in time $t - 1$ to unoccupied in time *t* (vacancy event). The model structure is as follows:

$Z_{i1} \sim \text{Bernoulli}(\psi_{i,1})$ for $i = 1, 2, ..., M$

$Z_{it} \sim \text{Bernoulli}(Z_{i,t-1}(1 - \varepsilon_{it}) + (1 - Z_{i,t-1})\gamma_{it})$ for $t = 2, 3, \ldots, T$

$Y_{ijt}|Z_{it} \sim \text{Bernoulli}(Z_{it}p)$ for $j = 1, 2, ..., J_i$

where Z_{i1} is the occupancy state (1 or 0) of site *i* during the first sampling occasion ($t = 1$, 'season 1'), Z_{it} is the occupancy state in subsequent sampling occasions ($t = 2, 3, \ldots, T$), and Y_{ijt} is the observed occurrence status (1 or 0) at site *i* in sub-count *j* during sampling occasion *t*. *M* is the total number of sample sites, *T* is the total number of sampling occasions, and *J* is the total number of sub-counts. We conducted three sub-counts (J = 3 X 3-min 20-sec sub-counts) during each sampling occasion ($T = 6$) at each sample site ($M = 183$ total sites). If site *i* is not occupied at time $t - 1$ ($Z_{i,t-1} = 0$), and the success probability of the Bernoulli is $0 * (1 - \varepsilon_{it}) + (1 - 0) * \gamma_{it}$, so the site is occupied (i.e., settled) in sampling occasion *t* with probability γ_{it}. Conversely, if site *i* is occupied in time $t - 1$ ($Z_{i,t-1} = 1$) and the success probability of the Bernoulli is given by $1 * (1 - \varepsilon_{it}) + (1 - 1) * \gamma_{it}$, the site remains occupied (i.e., does not become vacant) in sampling occasion *t* with probability $1 - \varepsilon_{it}$. It is important to note that colonization and extinction are not quantified in absolute terms; they are relative to the number of occupied and unoccupied sites in the previous sampling occasion. For example, if 20 of 100 sites were occupied in time $t - 1$ (20% occupied), with a vacancy rate of 30% and a settlement rate of 20%, 16 sites (20% of 80 unoccupied sites) would get settled, 6 sites (30% of 20 occupied sites) would be vacated, resulting in 30 sites being occupied in time *t* ($20*[1-0.3] + [100 - 20]*0.2 = 30$).

We estimated the four parameters (p, ψ, γ, and ε) using maximum likelihood techniques based on site detection histories (Y_{ijt}) with the following likelihood equation (MacKenzie *et al.*, 2003; Fiske & Chandler, 2011):

$$L(\psi_1, \varepsilon, \gamma, p|\{Y_{ijt}\}) = \prod_{i=1}^{M} \Pr(Y_{ijt})$$

Here, ψ_1 refers to the initial occupancy in the first sampling occasion, where thereafter ε and γ determine site occupancy in the following sampling occasions ('seasons'). *p* is the probability of detection given that site is occupied. Parameters can be modeled as a function of site- and survey-level covariates on the logit scale.

We calculated occupancy probability in time periods 2-6 using the following formula:

$$\psi_{t+1} = (1 - \psi_t) * \gamma + \psi_1 * (1 - \varepsilon)$$

which states that occupancy in time t+1 is the sum of the unoccupied sites that become colonized and the occupied sites that do not go extinct. It is important to note that colonization and extinction rates are always relative to the number of sites that are occupied in time t. The predicted distribution maps were created using this formula and the modeled relationships with covariates in the form of raster files.

Appendix S4. Methods for creating spatial maps of bird distributions as a function of microclimate and vegetation structure variables.

We created distribution maps for each species using the final model and maps of the microclimate and vegetation structure variables. The maps of the microclimate variables are the spatial predictions from boosted regression tree models created in Frey *et al.* (2016) at Science Advances. In that manuscript, we model local-scale, under-canopy air temperature as a function of elevation, microtopography, and vegetation structure. The importance of these predictors depended on the microclimate variable (some were more influenced by elevation, others by microtopography, and others by vegetation). The maps for the principal components (PC1 and PC2) were created using the raster layers of the LiDAR-derived vegetation variables and their respective contributions from the principal component analysis. The bird distributions were created by using raster layers (maps) for each variable category (microclimate and vegetation structure) as the input variables for the predicted estimates from the dynamic occupancy model (predict() function in 'unmarked' package in R). It is important to note that the actual temperature measurements were used as the predictor variables in the dynamic occupancy models. The predicted maps of the microclimate variables were only used to produce the bird distribution maps.

Appendix S5. Results from home range tests on assumptions of dynamic occupancy models.

We found no relationship between home range size and probability of settlement (neither in 2012 nor 2013) or with vacancy in 2013. However, in 2012 we did find a positive relationship between home range size and mean vacancy probability ($\hat{\beta}$ ± SE = 0.005 ± 0.002, $P = 0.052$, $r^2 = 0.204$) supporting the hypothesis that large home ranges might result in biases to dynamic occupancy estimates. This pattern was driven by the species with the largest home ranges (Steller's jay: 80ha; varied thrush: 7ha; and brown creeper: 4.2 ha). Mean home range size for the 12 remaining species was 1.2 ha [range = 0.3 – 2.8ha], Table 1). When these three outliers were removed from the sample, the relationship disappeared ($\hat{\beta}$ ± SE = 0.022 ± 0.015, $P = 0.16$, $r^2 = 0.11$) suggesting that this problem might exist only for species with home ranges much larger than the count circle (3.14ha).

Appendix S6. Dryad digital depository for AIC model selection tables.

All AIC model selection tables and associated coefficients at for 2012 and 2013 for all species can be found at the Dryad digital depository site:

http://dx.doi.org/10.5061/dryad.m35k6

Column names for the model coefficients use the following notation: coefficient = parameter(covariate) and standard error = SEparameter(covariate). Parameter abbreviations are p = detection probability, psi = initial occupancy, col = colonization/settlement, ext = extinction/vacancy. Parameter(Int) refers to the intercept. 'nPars' is the number of parameters estimated in the model. Each model is ranked by its AIC score, which represents how well the model fits the data. A lower ΔAIC (delta) value is indicative of a better model. The probability that the model (of the models tested) would best explain the data is indicated by AICwt.

Appendix S7. Methods for Breeding Bird Survey population trends comparison between cool- and warm-associated species.

We compared the Breeding Bird Survey (BBS) trends for the cool- and warm-associated species (see Table 1 for thermal preferences) to test whether cool-associated species were more likely to be declining in the region. We used the BBS trends for the 10-year period from 2002-2012 from the Pacific Northwest temperate rainforest region. We used the online regional trend analysis form (http://www.mbr-pwrc.usgs.gov/bbs/trend/tf13.html) to obtain the BBS trend estimates (see estimates below). The mean trend [95% CIs] for the cool-associated species was -1.06 %/year [-1.96 – -0.16]) and -0.16 %/year [-0.99 – 0.68] for the warm-associated species, indicating that the cool-associated species were in fact more likely to be declining when compared to their warm-associated counterparts.

Species	Thermal pref.	BBS trend 2002-12	LCL	UCL
BRCR	warm	0.19	-1.77	1.88
CBCH	warm	-1.94	-3.70	-0.23
GCKI	cool	-2.25	-3.68	-0.78
HAFL	warm	1.08	-0.55	2.71
HETH	cool	-0.77	-2.42	0.68
HEWA	cool	-0.07	-0.74	0.62
ORJU	cool	-1.36	-2.52	-0.34
PAWR	warm	1.80	0.36	3.27
PSFL	warm	-1.48	-2.78	-0.19
RBNU	cool	0.13	-1.75	2.05
STJA	warm	-0.42	-1.41	0.46
SWTH	warm	-0.67	-1.42	0.16
VATH	cool	-1.08	-3.18	1.28
WETA	warm	0.17	-0.34	0.67
WIWA	cool	-2.02	-2.57	-1.48

(a)

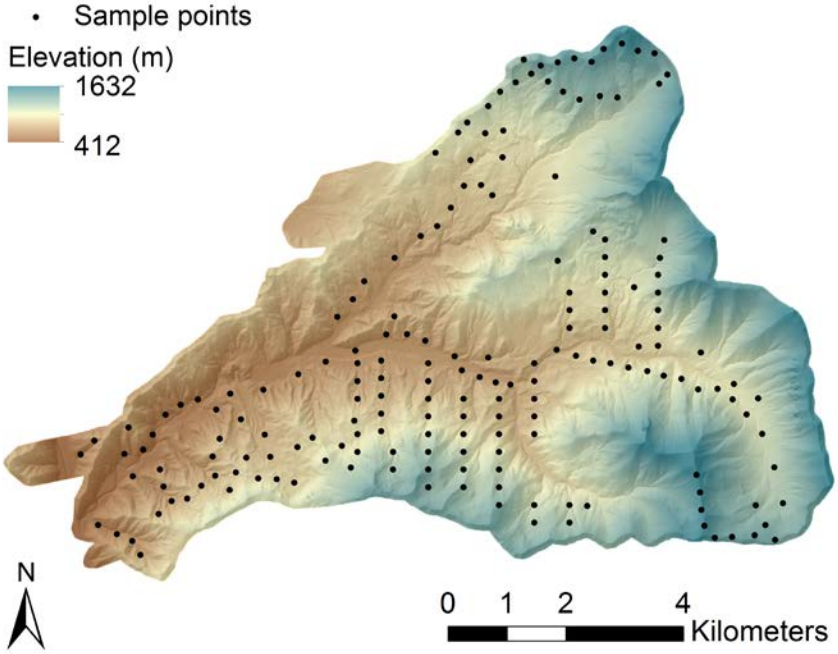
Sample points
Elevation (m)
1632
412
N
0
1
2
4
Kilometers

(b)

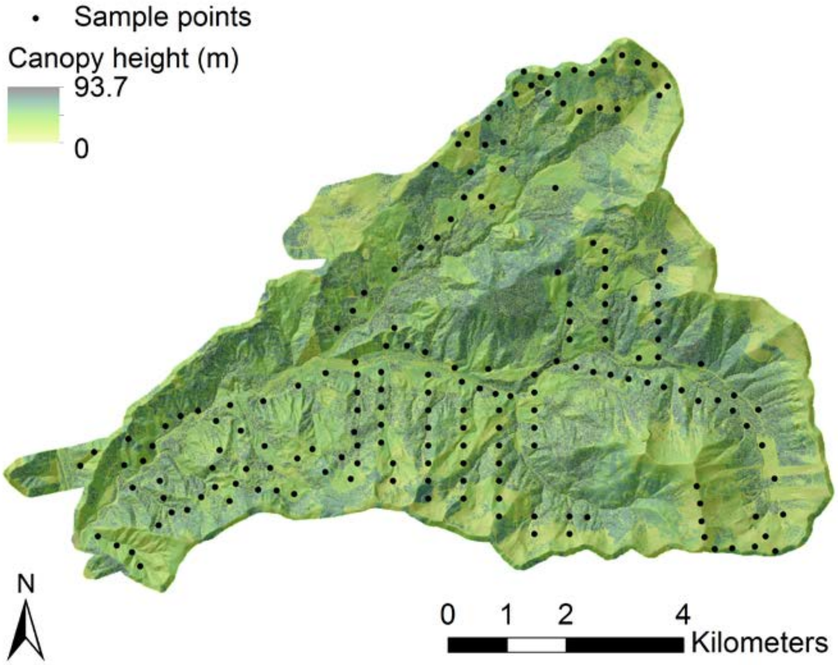
Sample points
Canopy height (m)
93.7
0
N
0
1
2
4
Kilometers

Figure S2. Maps of study area showing sample points, elevation gradient (a) and canopy height (b). We sampled birds at 183 point count stations across the H. J. Andrews Experimental Forest, Blue river, Oregon. Filled circles show sample points for both bird and temperature data. The gradient in elevation (low - orange to high – blue) is shown in meters. The canopy height is low (light green) to high (dark green). Hill shading reveals the underlying topography within the study area.

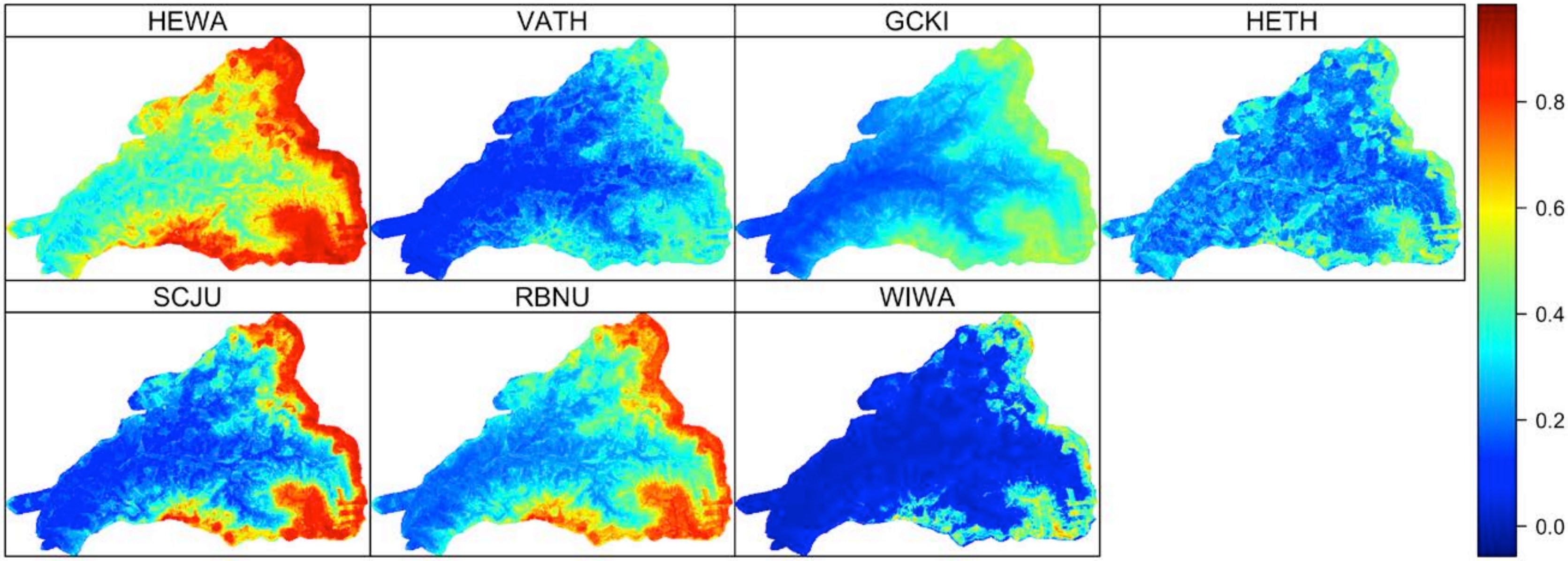

Figure S3. Predicted occupancy probability as a function of temperature and vegetation in the final sampling session of 2012 (session 6; late June to mid-July) for the cool-associated species. Blue = low occupancy probability, Red = high occupancy probability. See Table 1 for species codes. The Andrews Forest is low elevation to the east and high elevation to the west (see Fig. S2 for elevation gradient).

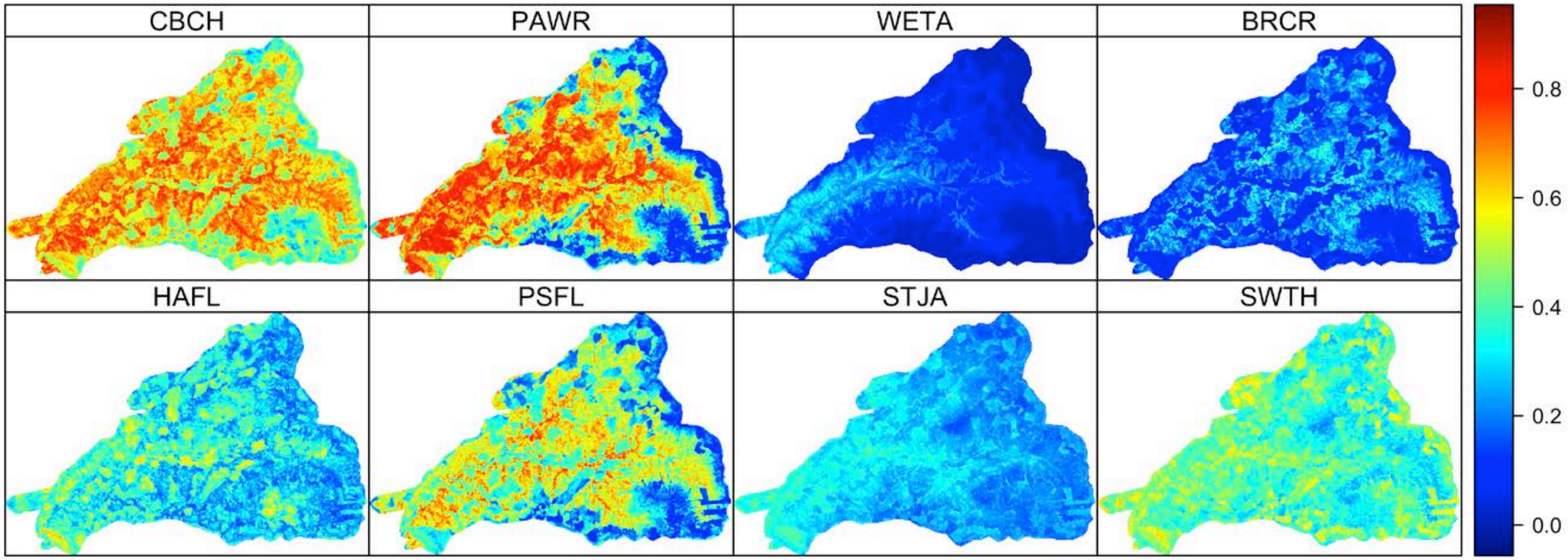

Figure S4. Predicted occupancy probability as a function of temperature and vegetation in the final sampling session of 2012 (session 6; late June to mid-July) for the warm-associated species. Blue = low occupancy probability, Red = high occupancy probability. See Table 1 for species codes. The Andrews Forest is low elevation to the east and high elevation to the west (see Fig. S2 for elevation gradient).

Table S3. Deciduous tree and large shrub species used to quantify forest composition at our sample points.

Common name	Scientific name
Big-leaf maple	*Acer macrophyllum*
Sitka alder	*Alnus viridis*
Beaked hazelnut	*Corylus cornuta*
Black cottonwood	*Populus tricocarpa*
Oregon white oak	*Quercus garryana*
Vine maple	*Acer circinatum*
Red alder	*Alnus rubra*
Pacific dogwood	*Cornus nutalli*
Cascara	*Rhamnus purshiana*
Bitter cherry	*Prunus emarginata*

Table S4. Pearson's correlation coefficients between all predictor variables (both temperature and vegetation structure).

	CDD >0 J-M	CDD >10 A-J	Max T A-J	Min T A-J	Mean T A-J	Veg str PC1	Veg str PC 2	Veg comp
CDD >0 J-M	1	0.79	0.57	0.70	0.70	0.15	0.19	-0.01
CDD >10 A-J	0.79	1	0.90	0.87	0.96	0.14	0.21	0.15
Max T A-J	0.57	0.90	1	0.70	0.89	0.01	0.16	0.31
Min T A-J	0.70	0.87	0.70	1	0.94	0.43	0.20	0.08
Mean T A-J	0.70	0.96	0.89	0.94	1	0.26	0.21	0.20
Veg str PC1	0.15	0.14	0.01	0.43	0.26	1	0.00	-0.29
Veg str PC 2	0.19	0.21	0.16	0.20	0.21	0.00	1	0.19
Veg comp	-0.01	0.15	0.31	0.08	0.20	-0.29	0.19	1

CDD = cumulative degree days, J-M = January – March, A-J = April – June, T = temperature, veg = vegetation, str = structure, comp = composition, PC = principal component.

Table S5. Coefficients (Est) and standard errors (SE) for initial occupancy (ψ) as a function of temperature and vegetation (structure and composition) metrics by species and year for top models. See Appendix S6 for all model selection tables. See Table 1 for definition of species codes.

			Vegetation									Temperature														
	Intercept		Structure PC1			Structure PC2			Composition			CDD >0 J-M			CDD >10 A-J			Max T A-J			Min T A-J			Mean T A-J		
Species	Est	SE	Est	SE		Est	SE		Est	SE		Est	SE		Est	SE		Est	SE		Est	SE		Est	SE	
2012																										
BRCR	-2.15	0.47							-1.71	0.82	**										0.60	0.30	**			
CBCH	0.59	0.21	0.30	0.22																	0.41	0.21	**			
GCKI	-1.34	0.22	-0.24	0.19														-0.80	0.22	**						
HAFL	-0.78	0.24				0.42	0.20	**	0.46	0.26	*							0.18	0.22							
HETH	-1.11	0.55							0.47	0.46		0.62	0.44													
HEWA	0.84	0.20	-0.17	0.20																				-0.58	0.21	**
ORJU	2.20	2.52	-1.21	1.10																	-3.25	2.64				
PAWR	0.23	0.17	0.24	0.19																	0.81	0.20	**			
PSFL	-0.73	0.19	0.16	0.22		-0.63	0.19	**	-0.27	0.24											0.88	0.24	**			
RBNU	-0.13	0.27				-0.56	0.25	**	-0.57	0.34	*													-0.67	0.26	**
STJA	-0.33	0.33	-0.49	0.29	*							0.52	0.32	*												
SWTH	-2.42	0.64							0.13	0.33		-0.93	0.53	*												
VATH	-1.36	0.25	-0.20	0.25																	-0.66	0.26	**			
WETA	-1.70	0.32	-0.29	0.29											0.55	0.27	**									
WIWA	-1.73	0.24	-0.45	0.23	**													-0.36	0.22							
2013																										
BRCR	-1.59	0.40				-0.40	0.26		-1.43	0.69	**							-0.58	0.32	*						
CBCH	-0.25	0.20				-0.38	0.19	**	-0.27	0.23														0.37	0.20	*
GCKI	-1.01	0.21				-0.22	0.21																	-1.46	0.24	**
HAFL	-1.58	0.26				0.08	0.21		0.64	0.22	**													1.05	0.27	**
HETH	-1.87	0.24							-0.38	0.32		0.16	0.22													
HEWA	1.17	0.20				-0.11	0.19																	-0.44	0.21	**
ORJU	-0.98	0.29	-0.38	0.26																	-0.38	0.25				
PAWR	0.04	0.18	0.55	0.20	**																0.38	0.19	**			
PSFL	-0.49	0.19	0.39	0.20	**	-0.37	0.17	**													0.98	0.24	**			
RBNU	0.95	0.27				-0.50	0.26	**				0.30	0.26													
STJA	1.20	0.59							-0.28	0.26														0.66	0.38	*
SWTH	-2.76	0.41				0.29	0.35		0.25	0.27																
VATH	-1.22	0.23				0.01	0.22					-0.73	0.22	**												
WETA	-3.39	0.71							1.34	0.51	**							1.25	0.62	**						
WIWA	-2.08	0.38				-0.29	0.30					-0.95	0.34	**												

** = 95% confidence interval does not overlap 0, * = 90% confidence interval does not overlap 0, CDD = cumulative degree days, J-M = January – March, A-J = April – June, T = temperature, PC = principal component.

Table S6. Coefficients (Est) and standard errors (SE) for detection probability (*p*) as a function of survey covariates by species and year for top models. Not all observers were not the same between years. Therefore, the comparison of detectability by observer is within years, not between years. Top models can also include temperature and vegetation metrics. These estimates are presented in Table S5. See Table 1 for definition of species codes. See Appendix S6 for all model selection tables.

	Intercept		Temporal autocov			Survey Time			Day of Year			Weather			Wind			Stream noise			Observer 2			Observer 3			Observer 4			Observer 5		Observer 6	
Species	Est	SE	Est	SE		Est	SE		Est	SE		Est	SE		Est	SE		Est	SE		Est	SE		Est	SE		Est	SE		Est	SE	Est	SE
2012																																	
BRCR	-0.70	0.27	1.12	0.29	**	-0.37	0.13	**										-0.36	0.12	**													
CBCH	-0.10	0.10	0.86	0.13	**							-0.12	0.06	**	-0.19	0.07	**	-0.26	0.06	**													
GCKI	0.16	0.15	0.67	0.18	**																												
HAFL	-0.72	0.30	1.45	0.29	**				-0.54	0.12	**							0.22	0.13	*	-0.38	0.70		-0.45	0.28	*	-1.41	0.29	**	1.02	1.28	0.05	0.32
HETH	-1.28	0.33	1.83	0.36	**	-0.02	0.12		0.68	0.15	**							-1.00	0.17	**													
HEWA	0.56	0.16	1.15	0.15	**							-0.16	0.07	**				-0.59	0.08	**	0.99	0.53	*	-0.71	0.18	**	-0.02	0.19		0.80	0.81	-0.13	0.18
ORJU	-0.96	0.17	1.66	0.20	**				0.99	0.09	**																						
PAWR	1.08	0.13	0.75	0.16	**	-0.40	0.07	**	0.16	0.07	**	-0.33	0.09	**																			
PSFL	0.38	0.13	0.75	0.16	**							-0.40	0.08	**																			
RBNU	-1.78	0.19	1.10	0.20	**				-0.45	0.09	**	-0.31	0.08	**				-1.08	0.14	**													
STJA	-0.74	0.33	0.68	0.27	**																0.92	0.44	**	-0.80	0.29	**	-0.57	0.27	**	-0.01	0.57	0.42	0.29
SWTH	-0.95	0.19	1.43	0.22	**	-0.56	0.09	**	0.95	0.15	**	-0.39	0.12	**																			
VATH	-0.33	0.22	0.93	0.24	**	-0.63	0.11	**																									
WETA	-0.96	0.28	0.54	0.32	*	-0.34	0.14	**										-0.51	0.18	**													
WIWA	0.25	0.25	0.74	0.29	**													-0.24	0.16														
2013																																	
BRCR	-0.71	0.24	1.15	0.26	**																												
CBCH	-0.57	0.18	0.90	0.16	**	-0.36	0.06	**													0.32	0.19	*	0.41	0.19	**	0.45	0.20	**				
GCKI	-0.14	0.20	0.56	0.17	**				-0.25	0.08	**				0.17	0.09	**				0.71	0.25	**	0.94	0.24	**	0.66	0.23	**				
HAFL	-0.77	0.29	1.53	0.30	**				-0.33	0.13	**							0.15	0.12		1.18	0.30	**	0.77	0.35	**	0.30	0.29					
HETH	0.86	0.21	0.63	0.24	**																-0.61	0.27	**	-0.63	0.29	**	-0.12	0.43					
HEWA	0.79	0.10	0.78	0.13	**										0.10	0.07		-0.51	0.07	**													
ORJU	-0.26	0.17	1.11	0.20	**	-0.24	0.08	**	0.48	0.09	**																						
PAWR	0.72	0.18	0.91	0.16	**	-0.31	0.07	**	0.30	0.08	**	-0.04	0.08								0.26	0.21		-0.20	0.22		0.47	0.23	**				
PSFL	0.21	0.15	0.81	0.14	**				-0.09	0.07											0.61	0.18	**	0.10	0.19		0.29	0.19					
RBNU	-0.56	0.11	1.20	0.14	**													-1.00	0.08	**													
STJA	-1.42	0.18	2.03	0.20	**	-0.16	0.07	**										-0.18	0.08	**	-0.24	0.17		-1.40	0.21	**	-0.90	0.19	**				
SWTH	0.04	0.27	0.91	0.25	**				0.53	0.17	**																						
VATH	-0.18	0.22	1.12	0.25	**	-0.41	0.12	**										-0.37	0.12	**													
WETA	-0.92	0.40	1.61	0.45	**																												
WIWA	-1.34	0.23	2.50	0.30	**	-0.03	0.11																										

** = 95% confidence interval does not overlap 0, * = 90% confidence interval does not overlap 0, CDD = cumulative degree days, J-M = January – March, A-J = April – June, T = temperature, PC = principal component.

Table S7. Coefficients (Est) and standard errors (SE) for detection probability (*p*) as a function of temperature and vegetation (structure and composition) metrics by species and year for top models. Top models can also include survey covariates. These estimates are presented in Table S6. See Table 1 for definition of species codes. See Appendix S6 for all model selection tables.

			Vegetation									Temperature														
	Intercept		Structure PC1			Structure PC2			Composition			CDD >0 J-M			CDD >10 A-J			Max T A-J			Min T A-J			Mean T A-J		
Species	Est	SE	Est	SE		Est	SE		Est	SE		Est	SE		Est	SE		Est	SE		Est	SE		Est	SE	
												2012														
BRCR	-0.70	0.27	0.24	0.21					-0.22	0.20																
CBCH	-0.10	0.10																						0.17	0.07	**
GCKI	0.16	0.15							-0.16	0.10	*				-0.39	0.11	**									
HAFL	-0.72	0.30				0.42	0.11	**	-0.07	0.10														0.38	0.13	**
HETH	-1.28	0.33																-0.59	0.15	**						
HEWA	0.56	0.16										0.28	0.07	**												
ORJU	-0.96	0.17	-0.30	0.10	**																0.07	0.11				
PAWR	1.08	0.13																								
PSFL	0.38	0.13	0.47	0.11	**				0.39	0.10	**										0.03	0.11				
RBNU	-1.78	0.19	-0.09	0.11	**				-0.27	0.14	*													-0.32	0.13	**
STJA	-0.74	0.33	-0.12	0.11																						
SWTH	-0.95	0.19				-0.01	0.10					-0.35	0.10	**												
VATH	-0.33	0.22	0.23	0.11	**										-0.32	0.14	**									
WETA	-0.96	0.28	-0.24	0.15		0.44	0.18	**				0.43	0.21	**												
WIWA	0.25	0.25																						0.44	0.22	**
												2013														
BRCR	-0.71	0.24	0.41	0.16	**				0.06	0.25											0.38	0.15	**			
CBCH	-0.57	0.18							-0.27	0.10	**													0.21	0.09	**
GCKI	-0.14	0.20													-0.32	0.11	**									
HAFL	-0.77	0.29																0.44	0.13	**						
HETH	0.86	0.21																			-0.16	0.10	*			
HEWA	0.79	0.10							-0.11	0.07	*													-0.08	0.07	
ORJU	-0.26	0.17																-0.15	0.09	*						
PAWR	0.72	0.18				-0.18	0.08	**																		
PSFL	0.21	0.15	0.13	0.08	*																0.25	0.09	**			
RBNU	-0.56	0.11	0.03	0.07																	-0.23	0.07	**			
STJA	-1.42	0.18	-0.09	0.09														0.15	0.09	*						
SWTH	0.04	0.27	-0.31	0.11	**																					
VATH	-0.18	0.22							-0.35	0.13	**							-0.14	0.12							
WETA	-0.92	0.40				0.22	0.15					0.58	0.14	**												
WIWA	-1.34	0.23	-0.35	0.14	**													-0.84	0.18	**						

** = 95% confidence interval does not overlap 0, * = 90% confidence interval does not overlap 0, CDD = cumulative degree days, J-M = January – March, A-J = April – June, T = temperature, PC = principal component.

Table S8. Coefficients (Est) and standard errors (SE) for all parameters from constant models. See Table 1 for definition of species codes.

	Detection		Occupancy		Colonization		Extinction	
Species	Est	SE	Est	SE	Est	SE	Est	SE
2012								
BRCR	0.587	0.028	0.261	0.058	0.202	0.031	0.608	0.074
CBCH	0.622	0.014	0.654	0.048	0.497	0.039	0.338	0.033
GCKI	0.675	0.018	0.292	0.043	0.284	0.026	0.511	0.042
HAFL	0.665	0.026	0.352	0.050	0.057	0.016	0.259	0.061
HETH	0.752	0.022	0.206	0.077	0.216	0.032	0.576	0.070
HEWA	0.782	0.010	0.703	0.042	0.364	0.032	0.264	0.026
ORJU	0.671	0.019	0.603	0.155	0.001	0.008	0.032	0.019
PAWR	0.836	0.009	0.558	0.038	0.316	0.025	0.278	0.031
PSFL	0.742	0.013	0.398	0.041	0.309	0.028	0.346	0.032
RBNU	0.482	0.023	0.577	0.066	0.119	0.034	0.094	0.038
STJA	0.438	0.027	0.428	0.072	0.260	0.038	0.717	0.064
SWTH	0.737	0.018	0.116	0.052	0.277	0.029	0.419	0.056
VATH	0.676	0.021	0.296	0.053	0.249	0.031	0.589	0.063
WETA	0.555	0.036	0.259	0.063	0.112	0.024	0.507	0.108
WIWA	0.628	0.032	0.225	0.045	0.037	0.011	0.241	0.073
2013								
BRCR	0.588	0.025	0.302	0.056	0.211	0.029	0.495	0.077
CBCH	0.607	0.016	0.472	0.051	0.340	0.032	0.353	0.047
GCKI	0.716	0.016	0.407	0.052	0.223	0.023	0.410	0.040
HAFL	0.768	0.018	0.406	0.069	0.096	0.019	0.265	0.061
HETH	0.725	0.020	0.143	0.028	0.150	0.015	0.587	0.070
HEWA	0.799	0.009	0.776	0.037	0.449	0.036	0.293	0.021
ORJU	0.664	0.018	0.301	0.058	0.227	0.028	0.351	0.093
PAWR	0.809	0.011	0.511	0.041	0.250	0.022	0.288	0.026
PSFL	0.740	0.012	0.477	0.045	0.380	0.032	0.261	0.031
RBNU	0.686	0.013	0.738	0.055	0.391	0.067	0.204	0.038
STJA	0.462	0.025	0.731	0.129	0.002	0.021	0.058	0.026
SWTH	0.737	0.017	0.064	0.022	0.241	0.020	0.449	0.043
VATH	0.704	0.021	0.265	0.043	0.204	0.022	0.731	0.046
WETA	0.629	0.034	0.085	0.026	0.125	0.022	0.830	0.056
WIWA	0.748	0.026	0.174	0.045	0.054	0.015	0.156	0.063

Table S9. Comparison of effect sizes between fine-scale temperature and vegetation for settlement and vacancy probability in the top models by species and year. See Table 1 for species codes.

	2012							
	Settlement				Vacancy			
Species	Veg Est/SE	Temp Est/SE	Abs diff	Larger effect	Veg Est/SE	Temp Est/SE	Abs diff	Larger effect
BRCR	3.98	0.00	3.98	Veg	1.41	0.00	1.41	Veg
CBCH	-3.01	2.13	0.88	Veg	-1.86	-1.70	0.16	Veg
GCKI	-1.18	-4.97	-3.79	Temp	0.66	2.04	-1.38	Temp
HAFL	2.11	-1.26	0.84	Veg	-1.73	-2.36	-0.63	Temp
HETH	-2.61	0.89	1.73	Veg	0.41	2.40	-1.98	Temp
HEWA	-1.15	-3.40	-2.25	Temp	1.32	2.58	-1.25	Temp
ORJU	-2.38	-2.86	-0.48	Temp	0.89	4.74	-3.85	Temp
PAWR	4.65	3.67	0.97	Veg	-2.25	-4.39	-2.15	Temp
PSFL	4.39	2.07	2.32	Veg	2.24	-1.26	0.98	Veg
RBNU	0.00	-1.16	-1.16	Temp	0.00	1.49	-1.49	Temp
STJA	-1.67	2.23	-0.57	Temp	-1.11	-0.91	0.21	Veg
SWTH	-1.94	1.81	0.13	Veg	1.07	0.00	1.07	Veg
VATH	-2.56	-4.02	-1.46	Temp	-0.14	2.61	-2.47	Temp
WETA	2.89	4.42	-1.53	Temp	1.68	-0.77	0.91	Veg
WIWA	-2.77	-2.25	0.52	Veg	0.94	3.49	-2.55	Temp
	2013							
BRCR	2.58	-1.56	1.02	Veg	1.69	-1.50	0.18	Veg
CBCH	-2.83	1.72	1.11	Veg	-2.18	-1.73	0.45	Veg
GCKI	-1.04	-6.79	-5.75	Temp	1.89	3.27	-1.37	Temp
HAFL	2.91	1.11	1.79	Veg	-2.07	-1.38	0.69	Veg
HETH	-3.93	-2.77	1.16	Veg	1.86	0.78	1.08	Veg
HEWA	-2.51	-3.92	-1.41	Temp	-0.59	4.00	-3.41	Temp
ORJU	-3.53	-3.60	-0.07	Temp	0.09	1.65	-1.56	Temp
PAWR	4.13	3.84	0.29	Veg	3.24	-3.28	-0.04	Temp
PSFL	3.45	3.46	-0.01	Temp	-2.27	-2.39	-0.12	Temp
RBNU	-2.03	-2.22	-0.20	Temp	1.07	1.58	-0.51	Temp
STJA	0.00	1.44	-1.44	Temp	0.00	1.28	-1.28	Temp
SWTH	1.78	3.41	-1.63	Temp	-2.20	-0.77	1.43	Veg
VATH	-1.71	-3.47	-1.76	Temp	-1.28	1.78	-0.50	Temp

WETA	-3.90	1.39	2.51	Veg	0.00	0.72	-0.72	Temp
WIWA	-2.49	-1.63	0.86	Veg	-1.97	-1.55	0.43	Veg

Est = estimate, SE = standard error, Veg = vegetation, Temp = temperature, Abs diff = absolute difference.

Table S10. Goodness-of-fit bootstrap results for top models of all species in 2012 and 2013. See Table 1 for definition of species codes.

Species	Obs	Mn BS	SD BS	Mn Obs - BS	Mn Obs - BS	*P*	No. sim
				2012			
BRCR	3178.86	3224.03	214.97	-45.17	214.97	0.54	250
CBCH	3140.72	3293.23	22.84	-152.50	22.84	1.00	250
GCKI	3149.57	3289.50	66.60	-139.93	66.60	0.98	250
HAFL	3145.32	3303.28	257.10	-157.96	257.10	0.70	250
HETH	2929.98	3306.93	300.91	-376.94	300.91	0.94	250
HEWA	2851.23	3297.28	36.53	-446.05	36.53	1.00	250
ORJU	3160.45	3238.05	123.96	-77.60	123.96	0.78	250
PAWR	2853.67	3291.20	59.92	-437.53	59.92	1.00	250
PSFL	3085.99	3289.16	84.78	-203.18	84.78	0.99	250
RBNU	2863.99	3299.70	502.15	-435.71	502.15	0.96	250
STJA	3313.38	3296.52	50.86	16.86	50.86	0.33	250
SWTH	2753.01	3241.17	297.53	-488.16	297.53	0.99	250
VATH	3039.51	3284.69	95.67	-245.18	95.67	1.00	250
WETA	3006.59	3259.89	538.26	-253.30	538.26	0.67	250
WIWA	3025.45	3290.73	177.33	-265.28	177.33	0.94	250
				2013			
BRCR	2960.58	3239.94	212.65	-279.36	212.65	0.97	250
CBCH	3176.44	3292.38	45.24	-115.94	45.24	0.98	250
GCKI	3160.40	3291.25	98.24	-130.84	98.24	0.93	250
HAFL	3146.81	3279.96	158.35	-133.15	158.35	0.78	250
HETH	3383.27	3283.91	79.92	99.36	79.92	0.10	250
HEWA	3017.91	3291.32	35.90	-273.40	35.90	1.00	250
ORJU	3180.79	3294.59	69.57	-113.80	69.57	0.94	250
PAWR	3040.74	3295.62	94.70	-254.88	94.70	1.00	250
PSFL	3083.74	3298.29	95.66	-214.55	95.66	1.00	250
RBNU	2871.31	3279.62	105.40	-408.30	105.40	1.00	250
STJA	3212.45	3307.01	143.46	-94.56	143.46	0.82	250
SWTH	2993.44	3260.54	120.80	-267.10	120.80	0.97	250
VATH	3041.48	3293.75	86.44	-252.26	86.44	1.00	250
WETA	2927.75	3227.14	397.19	-299.39	397.19	0.84	250
WIWA	2985.06	3260.00	395.22	-274.94	395.22	0.79	250

Mn = mean, SD = standard deviation, Obs = observed, BS = bootstrapped, No. sim = number of simulations.

Table S11. Results from tests for spatial autocorrelation in the residuals from the top models for all species in 2012 and 2013. See Table 1 for definition of species codes.

	2012		2013	
Species	Moran's *I*	*P*	Moran’s *I*	*P*
BRCR	0.003	0.244	0.010	0.203
CBCH	0.016	0.233	0.007	0.206
GCKI	0.003	0.275	-0.003	0.240
HAFL	0.002	0.251	0.001	0.328
HETH	-0.013	0.225	0.007	0.229
HEWA	-0.022	0.139	-0.009	0.244
ORJU	-0.004	0.304	-0.007	0.251
PAWR	0.002	0.264	0.007	0.215
PSFL	0.001	0.291	0.002	0.244
RBNU	-0.001	0.200	0.005	0.189
STJA	0.030	0.206	0.002	0.236
SWTH	-0.026	0.193	0.003	0.246
VATH	0.002	0.176	-0.017	0.234
WETA	-0.012	0.186	0.000	0.243
WIWA	-0.009	0.262	0.002	0.239

Table S12. Interactions between temperature and vegetation variables from the top models for occupancy, colonization and extinction. The most important temperature and vegetation variables are listed for each parameter, species, and year along with the interaction term and its associated *P*-value.

		Occupancy				Colonization				Extinction			
Species	Year	Temp	Veg	Interaction	*P*	Temp	Veg	Interaction	*P*	Temp	Veg	Interaction	*P*
BRCR	2012	Min	Comp	-1.30	0.03	NA	PC1	NA	NA	NA	PC2	NA	NA
	2013	Max	Comp	-0.37	0.16	Max	PC1	-0.13	0.43	CDD10aj	PC2	0.46	0.07
CBCH	2012	Min	PC1	0.10	0.63	Min	PC2	0.71	0.002	CDD0jm	PC1	-0.03	0.82
	2013	Mean	PC2	-0.08	0.71	Min	PC2	-0.02	0.92	Mean	Comp	0.40	0.11
GCKI	2012	Max	PC1	-0.20	0.39	Mean	Comp	-0.38	0.02	Mean	PC2	-0.08	0.64
	2013	Mean	PC2	-0.21	0.43	Mean	PC2	-0.27	0.09	Mean	Comp	-0.02	0.92
HAFL	2012	Max	PC2	0.23	0.26	CDD0jm	Comp	0.19	0.31	Max	PC1	0.63	0.08
	2013	Mean	Comp	0.37	0.25	Mean	PC1	-0.27	0.12	Mean	PC2	0.88	0.01
HETH	2012	CDD0jm	Comp	-0.23	0.53	Min	PC1	-0.19	0.20	Min	PC1	0.32	0.27
	2013	CDD0jm	Comp	0.10	0.78	Mean	PC1	-0.07	0.58	Mean	PC1	-0.23	0.26
HEWA	2012	Mean	PC1	-0.67	0.005	Mean	PC1	-0.73	0.001	Min	PC1	-0.04	0.83
	2013	Mean	PC2	-0.61	0.01	Mean	PC1	0.05	0.78	Mean	PC1	0.02	0.83
ORJU	2012	Min	PC1	-0.54	0.16	Mean	PC1	-0.54	0.16	Min	Comp	-0.20	0.39
	2013	Min	PC1	0.07	0.76	Min	PC1	-0.06	0.69	Min	PC1	-0.05	0.76
PAWR	2012	Min	PC1	-0.01	0.97	Min	PC1	-0.07	0.62	Min	PC1	0.03	0.84
	2013	Min	PC1	-0.14	0.47	Min	PC1	-0.28	0.07	Min	PC2	-0.07	0.68
PSFL	2012	Min	PC2	-0.38	0.12	Min	PC1	0.10	0.43	Min	PC2	-0.20	0.24
	2013	Min	PC2	-0.09	0.72	Min	PC1	0.05	0.71	Min	PC1	-0.06	0.72
RBNU	2012	Mean	PC2	-0.38	0.20	Min	NA	NA	NA	Mean	PC1	-0.30	0.43
	2013	CDD0jm	PC2	0.19	0.54	Max	PC2	-0.54	0.12	Mean	Comp	-0.09	0.63
STJA	2012	CDD0jm	PC1	0.36	0.26	Mean	PC1	-0.09	0.57	CDD0jm	Comp	0.54	0.27
	2013	Mean	Comp	-1.31	0.04	CDD0jm	NA	NA	NA	Min	PC1	0.17	0.71
SWTH	2012	CDD0jm	Comp	0.03	0.94	Max	PC1	-0.58	0.004	NA	PC1	NA	NA
	2013	NA	Comp	NA	NA	Max	Comp	-0.14	0.11	Max	Comp	0.02	0.87
VATH	2012	Min	PC1	-0.29	0.25	Mean	PC2	0.26	0.04	Max	PC1	0.48	0.07
	2013	CDD0jm	PC2	0.11	0.62	CDD10aj	PC2	-0.10	0.43	Min	Comp	0.82	0.06
WETA	2012	CDD10aj	PC1	-0.54	0.13	CDD10aj	PC2	0.25	0.23	Mean	PC1	-0.07	0.85
	2013	Max	Comp	-0.75	0.02	Max	PC1	0.38	0.03	Min	NA	NA	NA
WIWA	2012	Max	PC1	-0.15	0.53	CDD10aj	PC1	-0.16	0.39	CDD10aj	PC1	1.16	0.06
	2013	CCD0jm	PC2	-0.13	0.71	Max	PC2	0.30	0.24	Mean	PC2	-0.47	0.53

References

Fisher, R.A. (1936) The use of multiple measurements in taxonomic problems. *Annals of Eugenics*, **7**, 179–188.

Fiske, I. & Chandler, R. (2011) unmarked: An R package for fitting hierarchical models of wildlife occurrence and abundance. *Journal of Statistical Software*, **43**, 1-23.

Franklin, J.F., Spies, T.A., Pelt, R.V., Carey, A.B., Thornburgh, D.A., Berg, D.R., Lindenmayer, D.B., Harmon, M.E., Keeton, W.S., Shaw, D.C., Bible, K. & Chen, J. (2002) Disturbances and structural development of natural forest ecosystems with silvicultural implications, using Douglas-fir forests as an example. *Forest Ecology and Management*, **155**, 399-423.

Frey, S.J.K., Hadley, A.S., Johnson, S.L., Schulze, M., Jones, J.A. & Betts, M.G. (2016) Spatial models reveal microclimatic buffering capacity of old-growth forests. *Science Advances*, **2**, e1501392.

MacKenzie, D., Nichols, J., Hines, J., Knutson, M. & Franklin, A. (2003) Estimating site occupancy, colonization, and local extinction when a species is detected imperfectly. *Ecology*, **84**, 2200-2207.

Spies, T.A., Johnson, K.N., Burnett, K.M., Ohmann, J.L., McComb, B.C., Reeves, G.H., Bettinger, P., Kline, J.D. & Garber-Yonts, B. (2007) Cumulative ecological and socioeconomic effects of forest policies in Coastal Oregon. *Ecological Applications*, **17**, 5-17.